Zoological Journal of the Linnean Society, 2019, **186**, 46–75. With 17 figures.

The use of micro-computed tomography as a minimally invasive tool for anatomical study of bivalves (Mollusca: Bivalvia)

FABRIZIO MARCONDES MACHADO[1*], FLÁVIO DIAS PASSOS[1,2] and GONZALO GIRIBET[3]

[1]*Programa de Pós-Graduação em Biologia Animal, Universidade Estadual de Campinas (UNICAMP) CEP 13083–970, Campinas, SP, Brasil*
[2]*Departamento de Biologia Animal, Instituto de Biologia, Universidade Estadual de Campinas (UNICAMP) – Cx. Postal 6109, CEP 13083–970, Campinas, SP, Brasil*
[3]*Museum of Comparative Zoology & Department of Organismic and Evolutionary Biology, Harvard University, 26 Oxford Street, Cambridge, MA 02138, USA*

Received 1 February 2018; revised 23 June 2018; accepted for publication 11 July 2018

Micro-computed tomography or micro-CT is a minimally invasive technique capable of generating 2D images and 3D tomographic reconstructions of small-sized animals without destroying the physical specimens. The technique has been previously applied to the study of bivalves, and here we extend it to study the anatomy of eight anomalodesmatan species through the exclusive use of a tomographic approach. Freshly fixed and museum specimens of Anomalodesmata, one of the least understood clades of bivalves, were selected and scanned. Tomographic anatomical descriptions were generated for *Pandora pinna* (Pandoridae), *Lyonsia alvarezii* (Lyonsiidae), *Allogramma formosa* (Lyonsiellidae), *Trigonulina ornata* (Verticordiidae), *Poromya rostrata* (Poromyidae), *Cetoconcha spinosula*, *Cetoconcha* aff. *smithii* (Cetoconchidae) and *Cuspidaria glacialis* (Cuspidariidae). The main internal anatomical features often evaluated for anomalodesmatans were documented. The tomographic images allowed for a detailed description of anatomical structures, including the mantle, ctenidia, labial palps and siphons, as well as the digestive, reproductive and nervous systems. This non-destructive technique thus proved to be an efficient tool for describing the anatomy of bivalves. The potential of micro-CT in concert with the constant development of new scanners, bring fresh perspectives to the anatomical study of bivalves. *Poromya spinosula* is transferred to *Cetoconcha* and Cetoconchidae, as ***Cetoconcha spinosula*** (Thiele, 1912) **comb. nov.**

ADDITIONAL KEYWORDS: anatomy – Anomalodesmata – bivalve systematics – marine bivalves – micro-CT – 3D reconstructions – 2D tomographic sections.

INTRODUCTION

Bivalvia constitutes the second most diverse class of molluscs, with estimates of between 8000 and 20 000 known recent species (see Bieler *et al.*, 2013: table 1). Traditional knowledge on bivalve anatomy has been based on observations derived from dissections, histology and electron microscopy (e.g. Pelseneer, 1911; Atkins, 1937; Stasek, 1963; Knudsen, 1970; Yonge, 1982; Morton, 1985; Purchon, 1987), techniques commonly resulting in permanently altered samples – frequently referred to as 'invasive' techniques. These studies require sectioning (for histology or transmission electron microscopy), critical point drying and metallic coating (for scanning electron microscopy), or can result in nearly completely destroyed specimens (in the case of dissections), thus posing a major problem when limited specimens are available (Candás *et al.*, 2016).

In recent years, the use of X-ray micro-computed tomography (also known as micro-CT, µCT, high-resolution CT, X-ray micro-CT or microtomography) has allowed acquisition of 2D images and 3D reconstructions, greatly improving anatomical work, by conducting observations without destroying specimens and requiring only minor alteration through staining (e.g. Golding *et al.*, 2009; Kerbl *et al.*, 2013; Faulwetter

*Corresponding author. E-mail: fabriziomarcondes@yahoo.com.br
[Version of Record, published online 14 September 2018; urn:lsid:zoobank.org:pub:741CC8EA-67BE-4627-B941-C9E66E35972E]

et al., 2013a; Fernández *et al.*, 2014; Carbayo *et al.*, 2016; Tessler *et al.*, 2016; Parapar *et al.*, 2017). Micro-CT is fast and capable of generating sections in three planes (e.g. transversal, sagittal and frontal) from a single specimen, which is impossible in a histological approach (Golding & Jones, 2007; Candás *et al.*, 2016). Although this novel, minimally invasive tool has its limitations, as, for example, the ability to distinguish organs of similar density, it expands the possibilities for the study of internal tissues, consequently bringing a fresh perspective to the anatomical study of small and rare marine bivalves.

Among the major clades that make up Bivalvia, Anomalodesmata stands out for harbouring many rare species, since they often occur in deep waters and are usually restricted to highly specialized niches (e.g. Morton, 1985; Harper *et al.*, 2000; Allen, 2008; Bieler *et al.*, 2014; Machado *et al.*, 2017). With a wide range of morphological adaptations, this group also includes different body shapes and habitats, such as the enigmatic tube-dwellers, burrowers in soft sediments, cementing species and the deep-sea carnivorous species usually presenting a raptorial inhalant siphon, modified labial palps and ctenidia reduced to a septal muscle (Morton, 1985; Harper *et al.*, 2000). In addition, the difficulty in accessing the species of this group, both in the field and from museum collections, makes anomalodesmatans one of the least understood groups of marine bivalves (Harper *et al.*, 2006).

In this context, the main goal of this study was to explore the use of micro-CT as a non-destructive, minimally invasive tool for the anatomical study of marine bivalves. For this purpose, freshly fixed and museum specimens of eight anomalodesmatan species belonging to seven families were selected with the aim of providing anatomical examination of the main internal features commonly used for the description of this group of bivalves.

MATERIAL AND METHODS

Specimens

A specimen from each of eight anomalodesmatan species was used for micro-CT scanning, including: *Pandora pinna* (Montagu, 1803) and *Cuspidaria glacialis* (Sars G. O., 1878) collected in the 1960s, from the Malacology collection of the Museum of Comparative Zoology, Harvard University (MCZ), USA; *Poromya rostrata* Rehder, 1843 and *Cetoconcha* aff. *smithii* Dall, 1808, collected in the 1990s; and *Lyonsia alvarezii* d'Orbigny, 1846, *Poromya spinosula* Thiele, 1912, *Allogramma formosa* (Jeffreys, 1882) and *Trigonulina ornata* d'Orbigny, 1853, collected in the 2000s (freshly fixed specimens), deposited in the ZUEC (Museu de Zoologia da Universidade Estadual de Campinas), Brazil (Fig. 1). Table 1 provides an overview of the specimens employed for imaging, as well as GPS coordinates for the collecting localities, depth and specimen dimensions.

Contrast solution

The specimens were stained using a solution containing 0.3% phosphotungstic acid (PTA), with 3% dimethyl sulphoxide (DMSO) to increase cell membrane permeability, in 95% ethanol (protocol adapted from: Faulwetter *et al.*, 2013b; Fernández *et al.*, 2014). To compare the effectiveness of internal tissue contrast, two different PTA contrast solutions and protocols were tested: (1) elaborated from an initial concentration of 99.995% of acid (pure concentration), and (2) from an already diluted solution at a concentration of 10% of PTA. Once stained, the specimens were placed into small plastic tubes of 0.5 mL (for small specimens) and 1.5 mL (for larger specimens) submerged in ethanol (95% EtOH) and sealed with Parafilm (Pechiney Plastic Packaging Co., Chicago, Illinois, USA) to be scanned. In order, to increase absorption of the contrast solution by the internal tissues, some specimens had their shells previously removed. All specimens were scanned in full length, prioritizing the visualization of internal structures important for the anatomical description of anomalodesmatans.

Micro-computed tomography (image acquisition and datasets' storage)

Imaging was performed using two micro-CT *SkyScan* scanners (Bruker MicroCT, Kontich, Belgium), *SkyScan 1173* equipped with an X-ray source of 40–130 kV, Flat Panel sensor of 2240 × 2240 pixels and maximum detectability of 5 µm; and *SkyScan 1272* equipped with an X-ray source of 20–100 kV, Flat Panel sensor of 14450 × 14450 pixels and maximum detectability of 0.3–0.4 µm. Scanning parameters for these two micro-CT scanners were as follows: *SkyScan 1173*, source voltage = 35–123 kV, source current = 60–140 mA, exposure time = 350–3200 ms, frames averaged = 4–6, random movement = 10, filter = no, binning = no, flat field correction = on and scanning time = about 40–166 min; and *SkyScan 1272* source voltage = 35–70 kV, source current = 140–142 mA, exposure time = 658–3751 ms, frames averaged = 3–5, random movement = 10, filter = Al, binning = no, flat field correction = on, and scanning time = about 217–304 min. Images were reconstructed using the software Nrecon and processed with the software CTAnalyzer (http://bruker-microct.com/products/downloads.htm). DataViewer software was used for the visualization and interpretation of 2D serial tomographic sections. 2D image plates used inverse background to improve the sharpness and consequently the visualization of

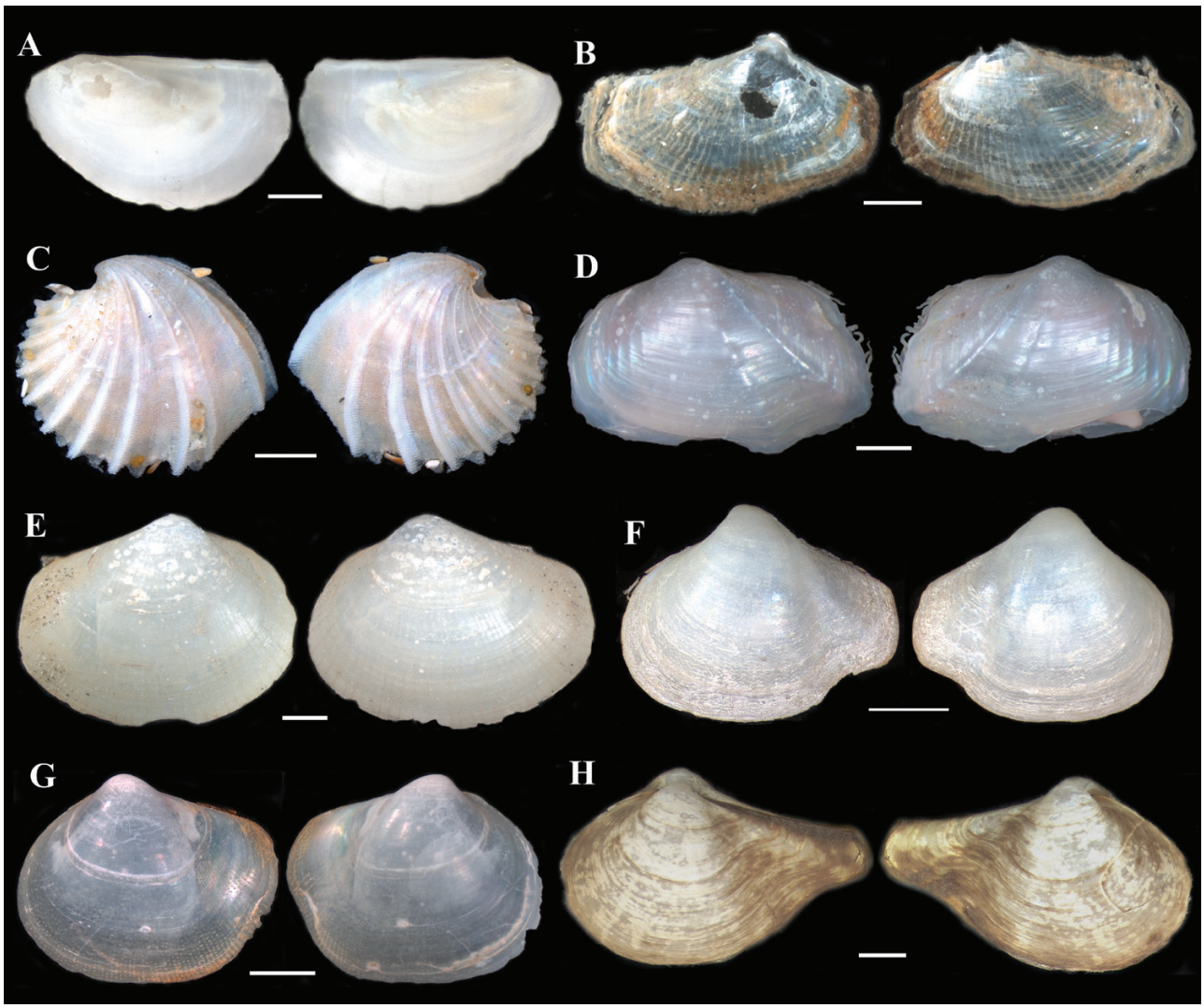

Figure 1. Shell photomicrographs of the specimens scanned. A, *Pandora pinna* (MCZ 375576). B, *Lyonsia alvarezii* (ZUEC 7005). C, *Trigonulina ornata* (ZUEC 7004). D, *Allogramma formosa* (ZUEC 7003). E, *Cetoconcha spinosula* **comb. nov.** (ZUEC 7002). F, *Poromya rostrata* (ZUEC 2243). G, *Cetoconcha* aff. *smithii* (ZUEC 2235). H, *Cuspidaria glacialis* (MCZ 388260). Scale bars: A, B, D–H = 2 mm, C = 1 mm.

the virtual sections. CTVox software was used for the 3D volume rendering and to assist in the virtual dissections. Density-based false-colour renderings were applied to the data in order to facilitate visualization of internal structures. In addition, all the volumetric datasets are on-line available at the Harvard's Dataverse under the link, https://dataverse.harvard.edu/dataverse/anomalodesmatamicroctdatasets.

Anatomical descriptions

Mantle, siphons, ctenidia, labial palps, musculature and the organs of the digestive, reproductive and nervous systems were documented and described, when possible. Some shell features (outline, thickness, outer sculpture and ligament) were also provided using a stereomicroscope. In order to put these species in a taxonomic context, a summary of the most up-to-date classification was provided (see Bieler *et al.*, 2014). In addition, it is worth noting that among the bivalves studied, only *Pandora pinna* (Pandoridae) and *Allogramma formosa* (Lyonsiellidae; as *Lyonsiella formosa*) had published detailed anatomical information (Allen, 1954; Allen & Turner, 1974; Morton, 1984a), while the other six species were largely unknown anatomically.

A list containing all abbreviations used in the figures is provided here following the terms commonly used in the anomalodesmatan literature (see: Yonge, 1952; Allen, 1954; Allen & Turner, 1974; Allen & Morgan, 1981; Morton, 1981, 1984a; Krylova, 1991, 2001; Bieler *et al.*,

Table 1. List of specimens used for micro-CT scanning. Abbreviations: GPS, Global Position System; EtOH, ethyl alcohol; m/mm, meters/millimetres; PTA, phosphotungstic acid; DMSO, dimethyl sulfoxide; kV, kilovolt/unit of voltage; µA, microampere/unit of electrical current; h/min/s, hours/minutes/seconds; µm, micrometre or 'micro' = 1×10^{-6} meter

Family	Species	Specimen data	Specimen dimensions	Contrast information	Scanning parameters
Pandoridae	*Pandora pinna* (Montagu, 1803)	MCZ 375576; collected July 1967; Bay of Biscay, Atlantic Ocean; GPS 47°40'N, 5°00'W; fixed in formalin, stored in 80% EtOH	1 mm diameter, 9 mm length	0.3% PTA-10% + 3% DMSO for 38 days.	*SkyScan 1173*, 106 kV, 60 µA, 41 min 9 s, 6.31 µm
Lyonsiidae	*Lyonsia alvarezii* d'Orbigny, 1846	ZUEC 7005; collected July 2014; Araçá Bay, São Paulo, Brazil; GPS 23º49′20″S, 45º24′10″W, 20 m; fixed in glutaraldehyde, stored in 95% EtOH	2.1 mm diameter, 6 mm length	0.3% PTA-99.9% + 3% DMSO for 3 days	*SkyScan 1272*, 37 kV, 140 µA, 3h 45 min 11 s, Al 1 mm, 4.24 µm
Lyonsiellidae	*Allogramma formosa* (Jeffreys, 1882)	ZUEC 7003; collected September 2013 on the continental slope, Argentina; GPS 37°49'39.6"S, 54°7'56.58"W, 1395 m; fixed and stored in 95% EtOH	5.8 mm diameter, 12.6 mm length	0.3% PTA- 10% + 3% DMSO for 38 days	*SkyScan 1173*, 123 kV, 63 µA, 1 h 2 min 14 s, 6.37µm
Verticordiidae	*Trigonulina ornata* d'Orbigny, 1853	ZUEC 7004; collected February 2009; Campos Basin, Rio de Janeiro, Brazil; GPS 22º55'7.5"S, 42º0'49.2"W, 29 m; fixed in formalin, stored in 70% EtOH	1 mm diameter, 3.2 mm length	0.3% PTA-99.9% + 3% DMSO for 3 days	*SkyScan 1272*, 35 kV, 140 µA, 5h 4 min 43 s, 4 µm
Poromyidae	*Poromya rostrata* Rehder, 1843	ZUEC 2243; collected January 1998; São Paulo, Brazil; GPS 25º43'90"S,45º09'50"W, 511 m; fixed in formalin, stored in 70% EtOH	2.2 mm diameter, 6.5 mm length	0.3% PTA-99.9% + 3% DMSO for 3 days	*SkyScan 1272*, 70 kV, 142 µA, 3h 40 min 17 s, Al 0.5 mm, 4.66 µm.
Cetoconchidae	*Cetoconcha spinosula* (Thiele, 1912) **comb. nov.**	ZUEC 7002; collected September 2013 on the continental slope, Argentina; GPS 37°49'39.6"S, 54°7'56.58"W, 1395 m; fixed and stored in 95% EtOH	4.6 mm diameter, 13.8 mm length	0.3% PTA-99.9% + 3% DMSO for 3 days	*SkyScan 1173*, 35 kV, 140 µA, 2h 46 min 40 s, 7.08 µm
Cetoconchidae	*Cetoconcha* aff. *smithii*	ZUEC 2235; collected September 1998; São Paulo, Brazil; GPS 24º20'53"S, 43º46'76"W, 505 m; fixed in formalin, stored in 70% EtOH	2.7 mm diameter, 7.1 mm length	0.3% PTA-99.9% + 3% DMSO for 3 days	*SkyScan 1272*, 70 kV, 142 µA, 3h 37 min 23 s, 5 µm
Cuspidariidae	*Cuspidaria glacialis* (Sars G. O., 1878)	MCZ 388260; collected June 1961; Gulf of Maine, Atlantic Ocean; GPS 43°0'N, 69°45'W, 3300 m; stored in 80% EtOH	3.5 mm diameter, 13 mm length	0.3% PTA-10% + 3% DMSO for 35 days	*SkyScan 1173*, 120 kV, 61 µA, 40 min 36 s, 8.14 µm

2014): an, anus; aam, anterior adductor muscle; aba, anterior branchial apertures; alp, anterior labial palp or anterior labial pouch; ao, anal opening; aod, ascending lamellae of outer demibranch; arm, anterior retractor muscle; asm, anterior septal muscle; bf, branchial filament; ba, branchial apertures; bs, branchial sieve slit; bt, byssal thread; ca, ctenidia axis; cae; gastric caecum; cg, circum-oesophagic ganglia; cs, crystalline style; ct, ctenidia; css, crystalline style sac; da, debris attached; de, debris; dg, digestive gland; did/dia, descending and ascending lamella of the inner demibranch; dod, descending lamella of outer demibranch; ea, exhalant siphonal aperture; es, exhalant siphon; f, foot; flp, fusion of the labial palp; fpo, fourth pallial opening; g, gut; gc, gastric chamber; go, gonad; gs, gastric shield; gsp1-3, grouped septal pores; h, heart/pericardium; ha, haemocoel space; hg, hindgut; hs, hollow sac; ia, inhalant siphonal aperture; ibc, infra-branchial chamber; id, inner demibranch; ilj, interlamellar junctions; is, inhalant siphon; isc, infraseptal chamber; k, kidney; li, lithodesma (calcified ligament); lp, labial palp; lsm, lateral septal muscle; mfg, marginal food groove; mg, midgut; mo, mouth; mm, mantle margin; mmf, mantle margin fusion; mmg, mantle margin glands; nb, nervous bundles; oa, ostial aperture; o, oesophagus; od, outer demibranch; og, oesophagus grooves; op, ostial perforations; ov, ovary; p, prey inside stomach; pam, posterior adductor muscle; pba, posterior branchial apertures; pg. pedal ganglia; plp, posterior labial palp or posterior labial pouch; po, pedal opening; prm, posterior retractor muscle; psm, posterior septal muscle; s, shell; sbc, supra-branchial chamber; sep, septum; sg, stomach grooves; si, siphons; sit, siphonal tentacle; sm, siphonal musculature; sph, sphincter; sp1-5, septal pores; ssc, supraseptal chamber; st, stomach; t, testis; ty, typhlosole; ulp, unfused labial palps; vg, visceral ganglia; vm, visceral mass;?, unknown structure (maybe an accessory muscle).

RESULTS

The 3D tomographic reconstructions were able to reproduce all major anatomical structures (siphons, ctenidia, labial palps, etc.) of the eight specimens analysed with high fidelity, highlighting the usefulness of the technique for the visualization and interpretation of internal organs. In contrast, for some minute organs of the visceral mass (small ganglia, kidney and heart), the 3D reconstructions were not very accurate, and some could not be clearly visualized. For these small organs visualization was only possible through the 2D tomographic sections. Anatomical structures measuring less than 3 µm, e.g. mantle margin glands, statocysts and gametes, were not discernible with the micro-CT scanners used for this study.

Below we provide the anatomical description of the species with two anatomical plates each including (1) 2D tomographic images, with transverse, sagittal and frontal sections, and (2) 3D renderings, showing the virtual dissections.

SYSTEMATICS

CLASS BIVALVIA LINNAEUS, 1758

SUBCLASS HETERODONTA NEUMAYR, 1884

INFRACLASS EUHETERODONTA GIRIBET & DISTEL, 2003

SUPERORDER ANOMALODESMATA DALL, 1889

FAMILY PANDORIDAE RAFINESQUE, 1815

GENUS *PANDORA* BRUGUIÈRE, 1797

PANDORA PINNA (MONTAGU, 1803)

(FIGS 2, 3)

Description

Shell: Subquadrate to subovate, robust, very compressed, strongly inaequivalve with left valve inflated and right valve flat or slightly concave; lithodesma absent.

Mantle: Mantle margin fused forming a short anterior pedal aperture and posteriorly with two short and very similar siphons; fourth pallial aperture absent.

Siphons: Inhalant and exhalant siphons similar in size and outline, simple tube-shaped, fused almost until the tip but not covered with periostracum; apertures of the inhalant and exhalant siphons fringed with a ring of, respectively, ~18 and ~16 short tentacles.

Ctenidia: Eulamellibranch and plicate; complete with a large inner demibranch and a much reduced outer demibranch consisting only of reflected descending lamellae; presence of a marginal food groove on the inner demibranch.

Labial palps: Large, wide, lamellate with sorting ridges, complete and symmetrical (typically bivalve plan).

Musculature: Adductor muscles present, well developed, posterior slightly larger than anterior; presence of poorly developed posterior and anterior pedal retractor muscles.

Foot: Well developed with a large pedal groove.

Digestive system: Presence of a tube-shaped mouth, long and thin oesophagus, small and rounded-shaped stomach with a short anterodorsal extension; stomach associated with the long crystalline style sac; crystalline style not visible in the specimen analysed;

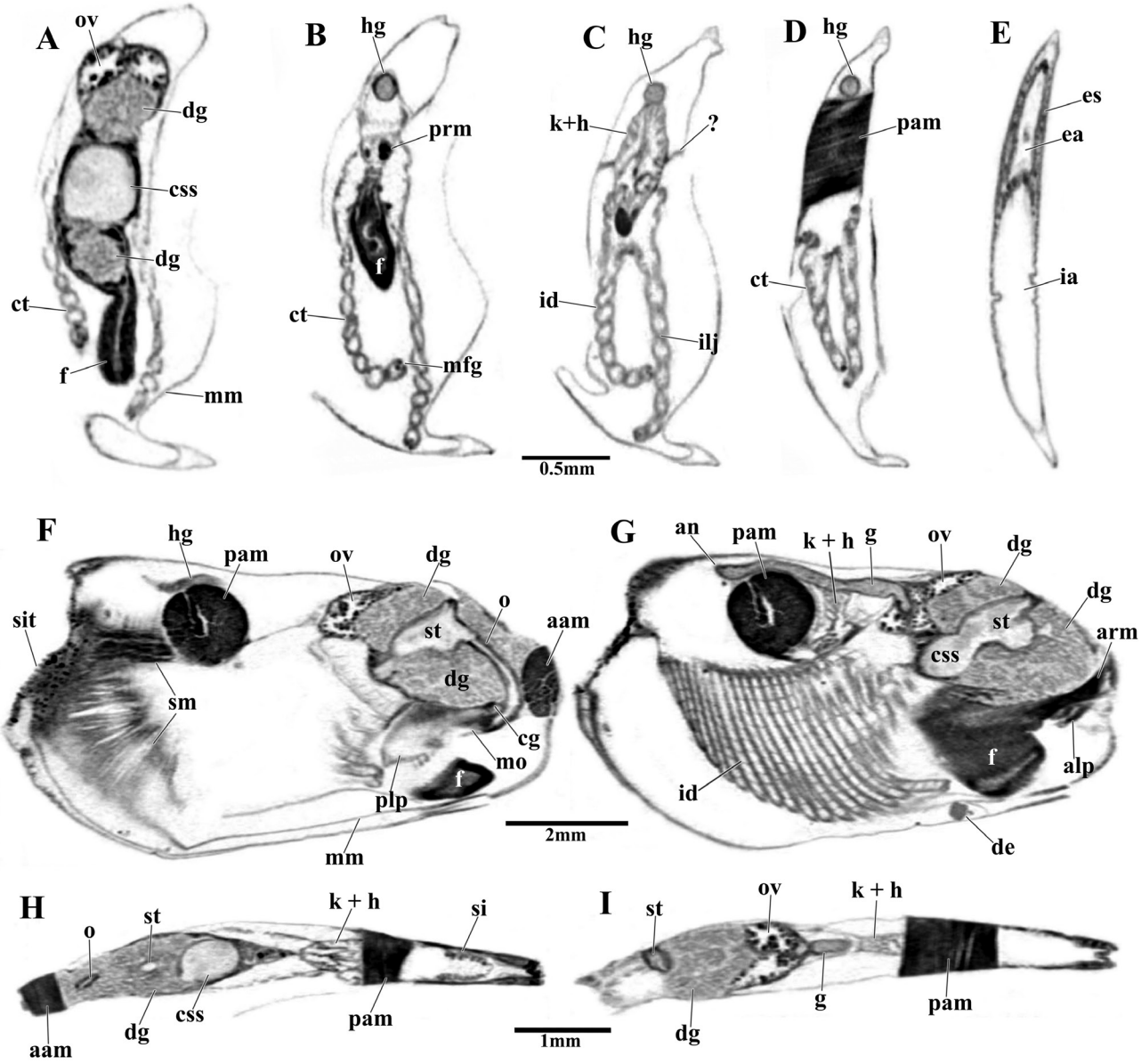

Figure 2. Selected virtual 2D sections through the micro-CT dataset of a PTA-stained specimen of *Pandora pinna*. Transverse (A–E), sagittal (F, G) and frontal (H, I) sections. Scale bars: A–E = 0.5 mm; F, G = 2 mm; H, I = 1 mm.

style sac conjoined with the midgut; pericardium/heart surround the rectum/hindgut and kidney, rectum passing over the posterior adductor muscle and ending in the anus.

Organs of the visceral mass: Heart + kidney apparently supported by a thin accessory muscle.

Reproductive system: Hermaphroditic, the ovary and testis are located in the dorsal portion of the visceral mass closely associated to the digestive gland, a small testicular mass is positioned below the ovary and was observed only through 3D reconstructions.

Nervous system: Presence of circum-oesophagic (cerebro-pleural) and visceral ganglia; pedal ganglia and statocysts not visible.

Family Lyonsiidae P. Fischer, 1887
Genus *Lyonsia* Turton, 1822
Lyonsia alvarezii d'Orbigny, 1846
(Figs 4, 5)

Description

Shell: Subovate-elongated, thin, delicate, translucid, moderately inflated in the anterior, posterior laterally

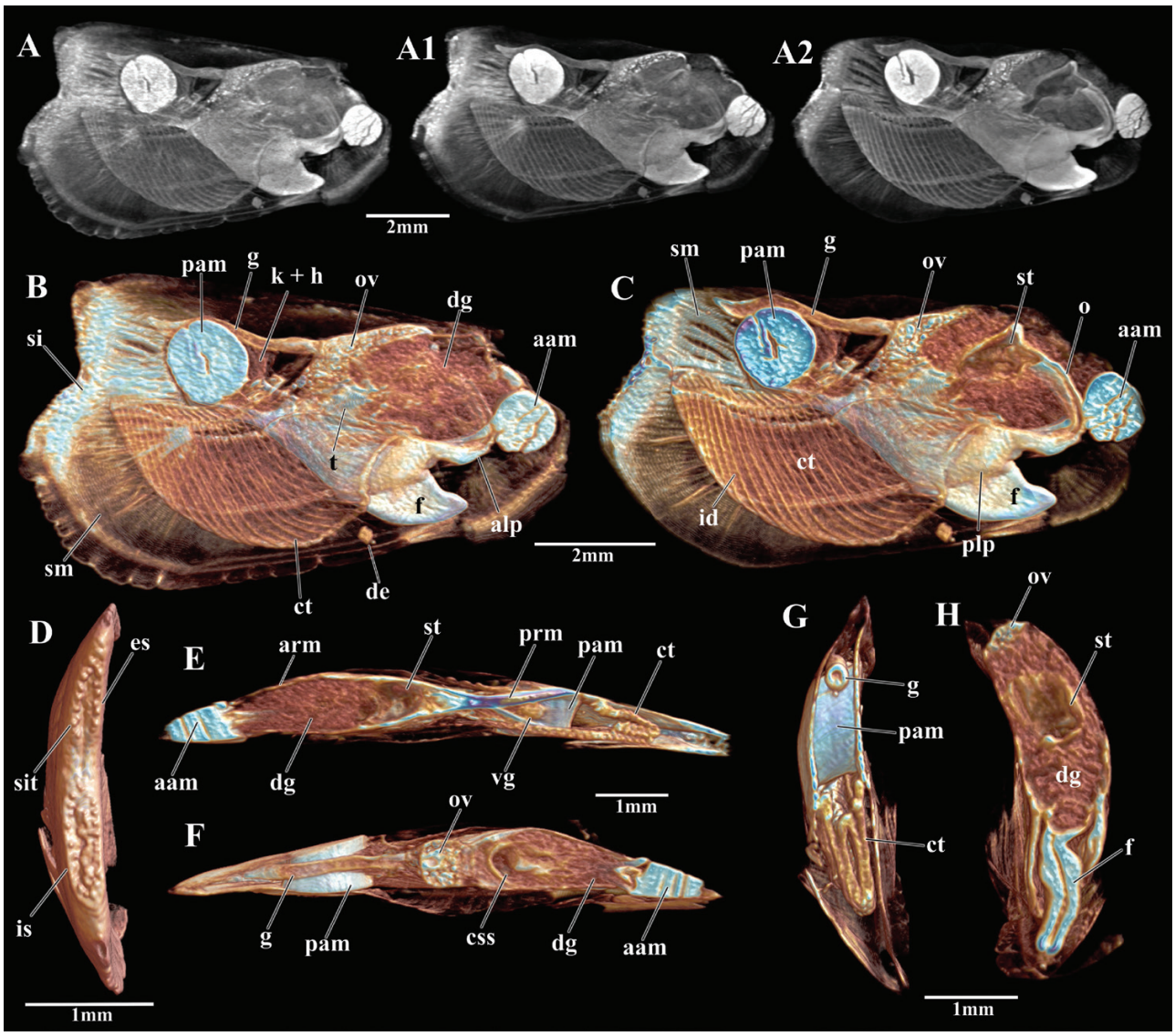

Figure 3. 3D volume rendering based on the micro-CT dataset of *Pandora pinna*, displaying internal organs. Dissection sequence in original tomographic colour, lateral view (A–A2); false-colour volume rendering in lateral view (B) and virtual dissections in sagittal (C), transverse (D, G, H) and frontal (E, F) sections. Scale bars: A–C = 2 mm; D–H = 1 mm.

compressed; external sculpture formed by thin radial ridges with sand grains attached along the entire extension of the valves; with a large lithodesma.

Mantle: This specimen had an important part of the mantle lost during the removal of the shell, turning the analysis incomplete; presence of a fourth pallial aperture closer to the inhalant aperture.

Siphons: Inhalant and exhalant siphons similar in size and outline, short, simple, tube-shaped and separated; papillate tentacles covering the inhalant siphon; apertures of the inhalant and exhalant fringed with a ring of, respectively, ~32 and ~45 short tentacles.

Ctenidia: Eulamellibranch and plicate; complete with a large inner demibranch larger than the outer one; free edge of inner demibranch with a deep marginal food groove.

Labial palps: Large, wide, lamellate with sorting ridges, symmetrical and coiled.

Musculature: Adductor muscles present, heteromyarian, with the posterior adductor well developed and the anterior reduced; presence of well-developed posterior and a reduced anterior pedal retractor muscle.

Foot: Elongated with a long pedal groove; presence of byssal thread.

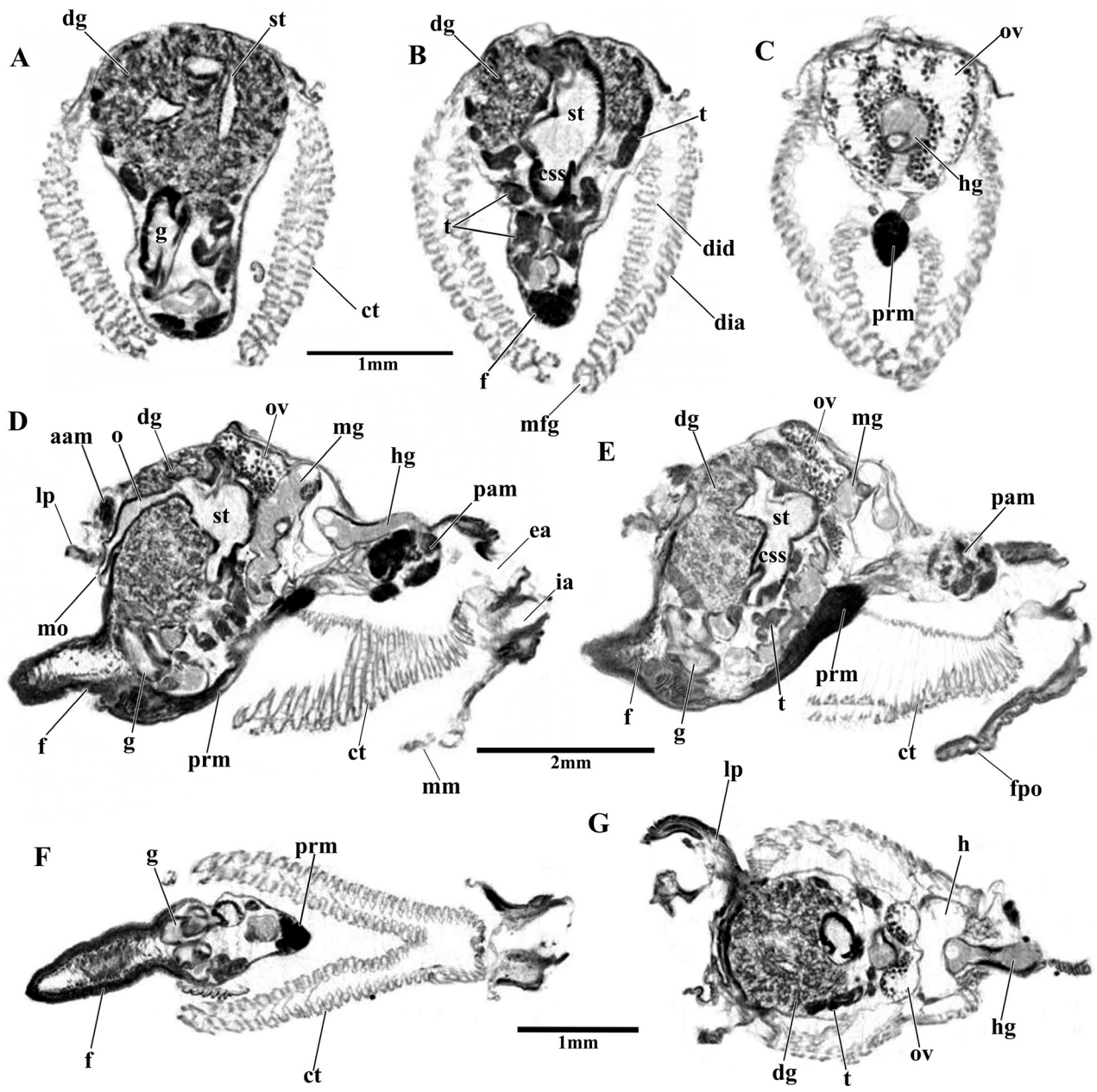

Figure 4. Selected virtual 2D sections through the micro-CT dataset of a PTA-stained specimen of *Lyonsia alvarezii*. Transverse (A–C), sagittal (D, E) and frontal (F, G) sections. Scale bars: A–C, F, G = 1 mm; D, E = 2 mm.

Digestive system: The tube-shaped mouth opens into a long oesophagus that enters into the anterior portion of the stomach; elongated in shape, the stomach is connected to the also elongated crystalline style sac; style sac conjoined with an anterior coiled midgut; pericardium/heart surround the rectum/hindgut; kidney not visible.

Reproductive system: Hermaphroditic; ovary located in the dorsal portion of the visceral mass, closely associated to the digestive gland; testis small and poor visible, located in the anterior portion of visceral mass.

Nervous system: Ganglia not visible.

Family Lyonsiellidae Dall, 1895

Genus *Allogramma* Dall, 1903

Allogramma formosa (Jeffreys, 1882)

(Figs 6, 7)

Description

Shell: Subquadrate, inflated, equivalve and inaequilateral; extremely fragile, pearl lustre; outer sculpture well

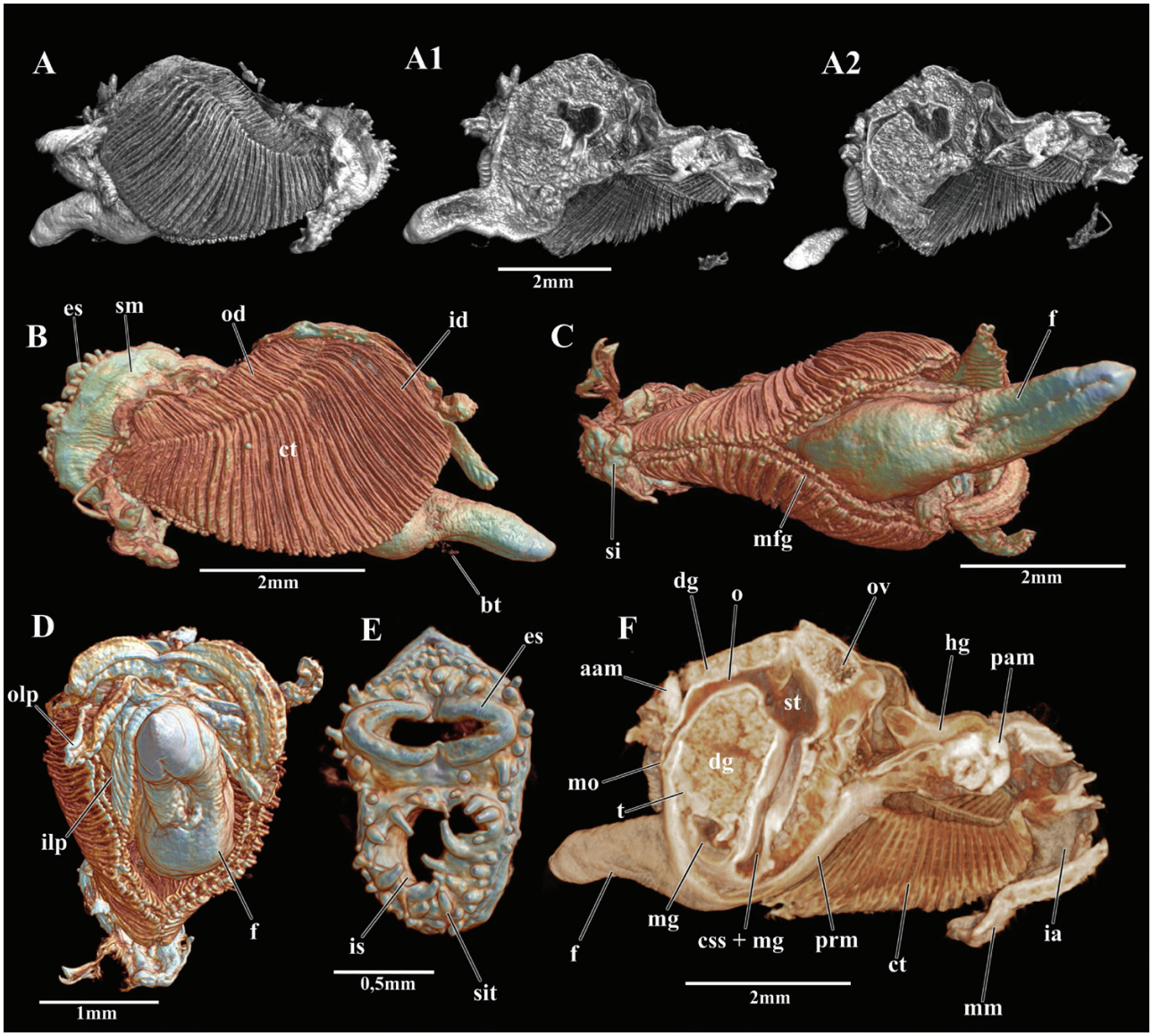

Figure 5. 3D volume rendering based on the micro-CT dataset of *Lyonsia alvarezii*, displaying internal organs. Dissection sequence in original tomographic colour, lateral view (A–A2); false-colour volume rendering in lateral (B), ventral (C) and anterior (D) view; virtual dissections in transverse (E) and sagittal (F) sections. Scale bars: A–C, F = 2 mm; D = 1 mm; E = 0.5 mm.

marked with two long radial ridges from the umbo until the posterior ventral margin of the valves, small spines in the posterodorsal portion of the shell; with a lithodesma.

Mantle: Mantle margin with two fused points, anteriorly forming a wide pedal gape and posteriorly forming the siphons; posteroventrally, mantle margin fusion formed by inner and middle folds (Type B) (Yonge, 1982); absence of a fourth pallial aperture.

Siphons: Separated, different in size and outline; inhalant siphon, large, modified in a raptorial appendage, usually contracted into the pallial cavity; exhalant siphon short, tube-shaped; both surrounded at the base by a ring of ~50 smaller tentacles closest to the aperture and by ~60 bigger tentacles peripherally located.

Ctenidia: Eulamellibranch, very reduced, non-plicate and horizontally aligned; complete, with two demibranchs.

Labial palps: Non-lamellate, extremely complex, outer and inner palps medially fused forming two pouches or buccal sacs, one small anterior and another large posterior; unfused tips forming narrow fluted funnels laterally.

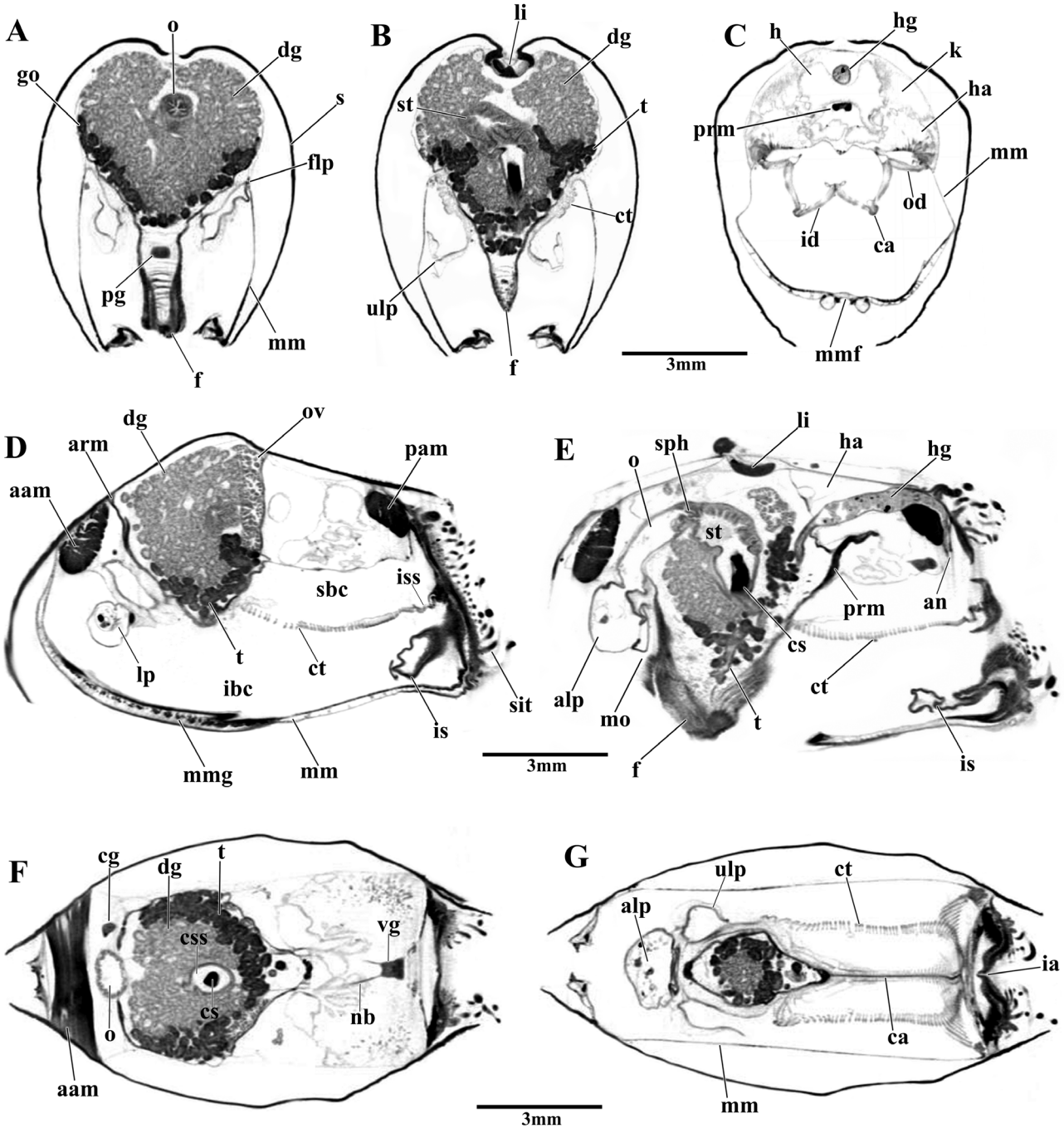

Figure 6. Selected virtual 2D sections through the micro-CT dataset of a PTA-stained specimen of *Allogramma formosa*. Transverse (A–C), sagittal (D, E) and frontal (F, G) sections. Scale bars: A–G = 3 mm.

Musculature: Posterior and anterior adductor muscles present and isomyarian; with posterior and anterior pedal retractor muscle; absence of taenioid muscle.

Foot: Large and elongated; absence of byssal thread.

Digestive system: Funnel-shaped mouth opening into a thick and muscular oesophagus that enters into the anterodorsal portion of the stomach; sphincter present between the oesophagus and the stomach; stomach small, rounded, with internal longitudinal grooves in the dorsal wall, connected to the large crystalline style sac and surrounded dorsally and anteriorly by the gonads and the digestive gland; style sac conjoined with an anterior coiled midgut; with a crystalline style; pericardium/heart surround the rectum/hindgut and the kidney.

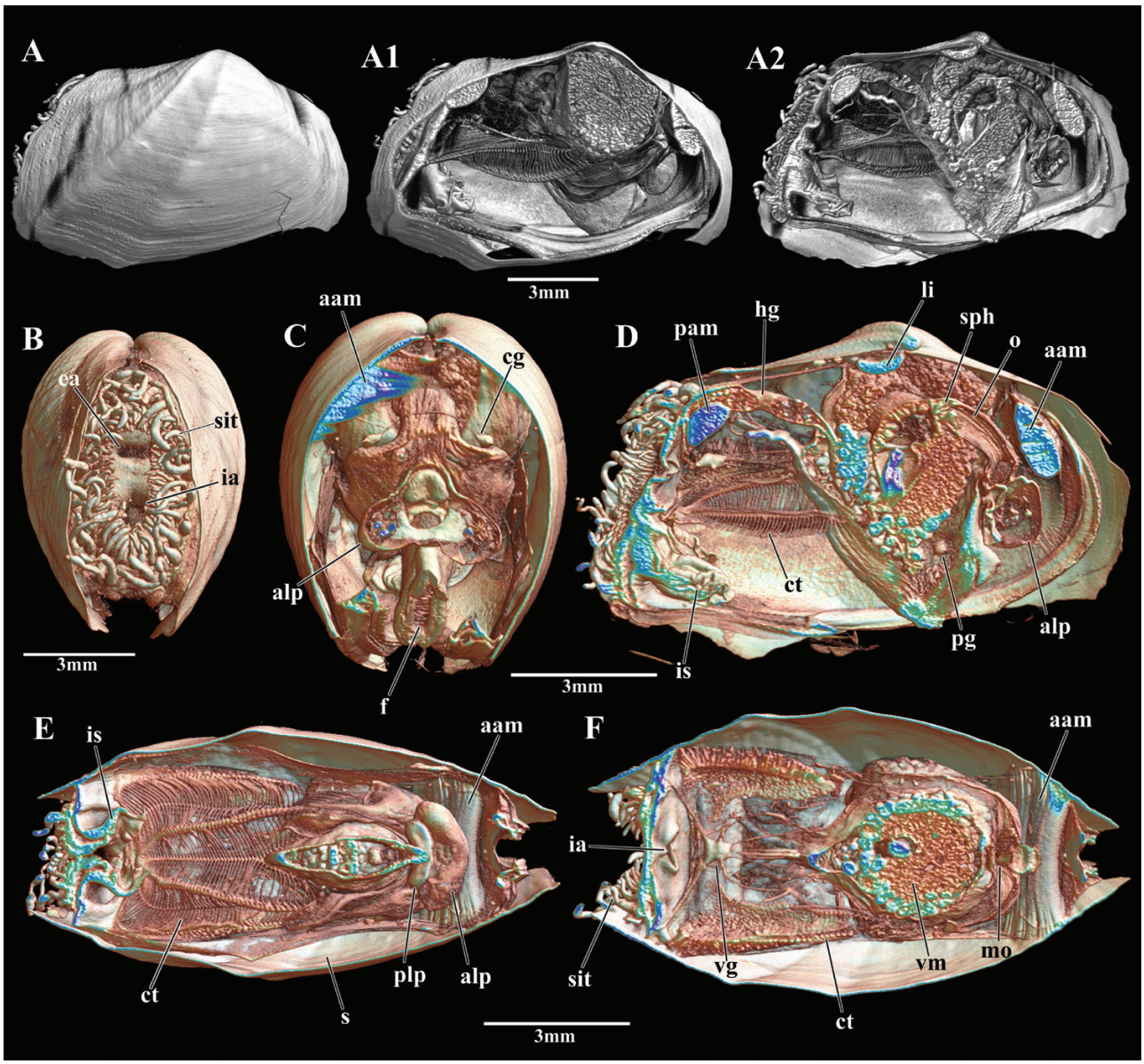

Figure 7. 3D volume rendering based on the micro-CT dataset of *Allogramma formosa*, displaying internal organs. Dissection sequence in original tomographic colour, lateral view (A–A2); false-colour volume rendering, posterior view (B), virtual dissections in transverse (C), sagittal (D) and frontal (E, F) sections. Scale bars: A–F = 3 mm.

Organs of visceral mass: A lacunar system formed by haemocoel spaces is present in the posterior portion of the visceral mass, associated with the kidney and heart.

Reproductive system: Hermaphroditic, ovary and testis well visible, closely associated to the digestive gland; ovary dorsally located and testis in the anteroventral portion of visceral mass penetrating partially into the foot.

Nervous system: With visible circum-oesophagic, pedal and visceral ganglia; nervous bundles of visceral ganglia branching into the siphons, visceral mass and ctenidia.

FAMILY VERTICORDIIDAE STOLICZKA, 1870

GENUS *TRIGONULINA* D'ORBIGNY, 1853

TRIGONULINA ORNATA D'ORBIGNY, 1853

(FIGS 8, 9)

Description

Shell: Oval, compressed, robust; external sculpture formed by prominent and irregularly spaced radial ribs; lunule deeply impressed; debris attached by the entire length of outer surface of the valves; lithodesma present.

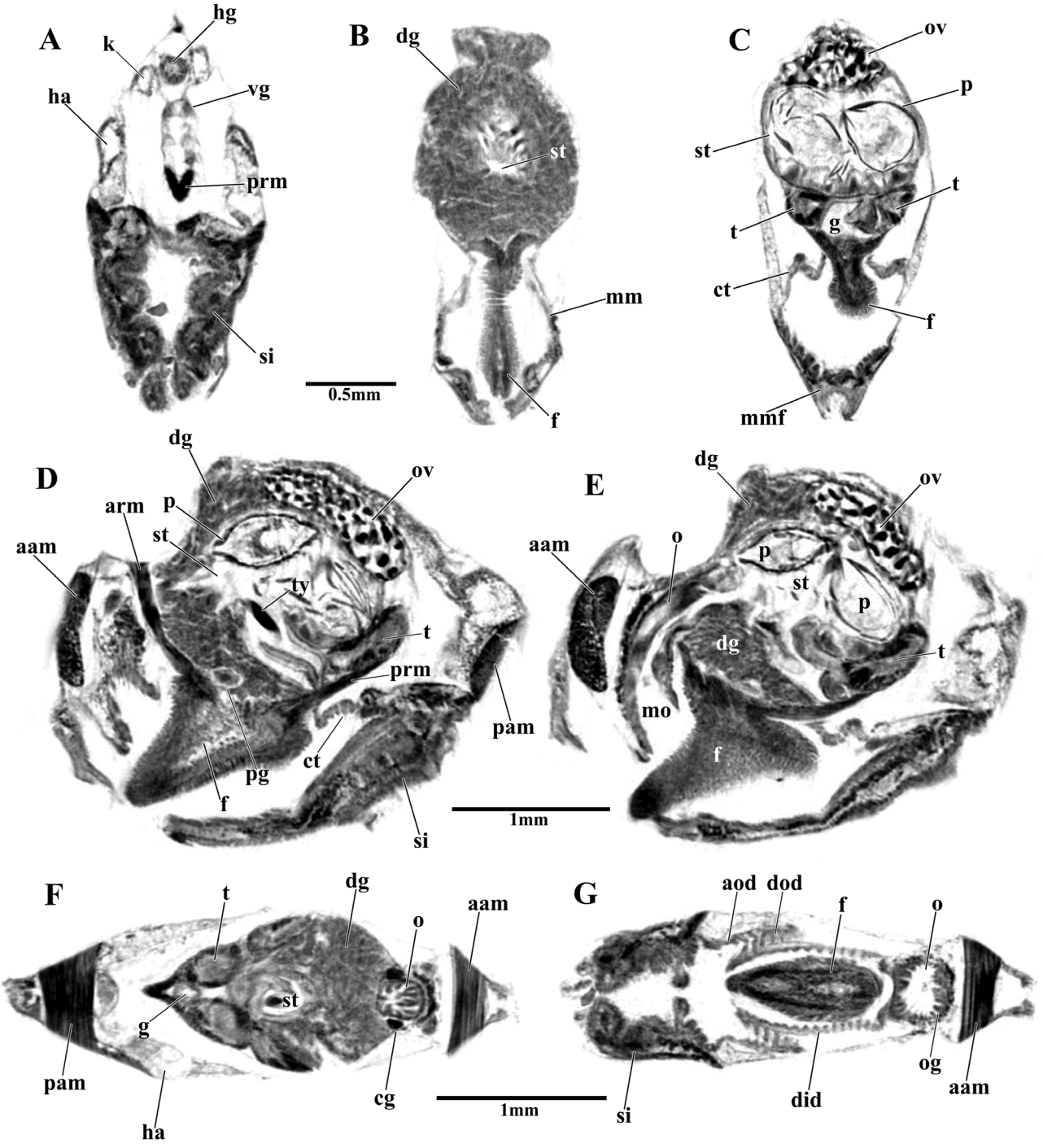

Figure 8. Selected virtual 2D sections through the micro-CT dataset of a PTA-stained specimen of *Trigonulina ornata*. Transverse (A–C), sagittal (D, E) and frontal (F, G) sections. Scale bars: A–C = 0.5 mm; D–G = 1 mm.

Mantle: Mantle margin mostly unfused anteriorly forming a large pedal aperture; posteriorly there is a ventral fusion forming the siphons; without a fourth pallial aperture.

Siphons: Separated; inhalant siphon, muscular, short, thin, cone-shaped, contracted into the pallial cavity; exhalant, very small, barely visible; siphonal apertures surrounded at their base by siphonal tentacles, ~20 around the inhalant and three around the exhalant aperture.

Ctenidia: Highly reduced, non-plicate and horizontally aligned; complete, with inner and reduced outer

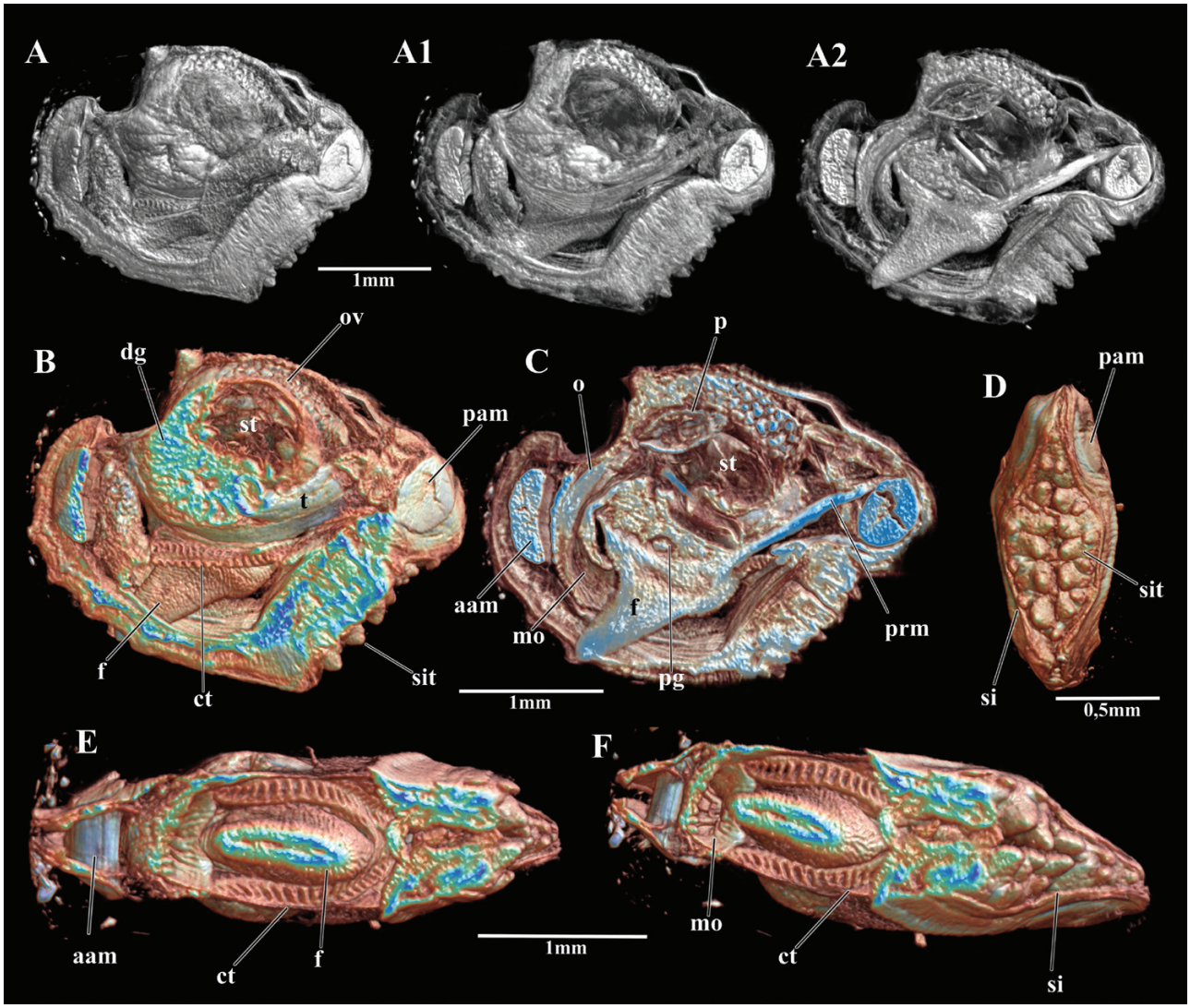

Figure 9. 3D volume rendering based on the micro-CT dataset of *Trigonulina ornata*, displaying internal organs. Dissection sequence in original tomographic colour, lateral view (A–A2); false-colour volume rendering, virtual dissections in sagittal (B, C), transverse (D) and frontal (E, F) sections. Scale bars: A–F = 1 mm.

demibranchs, extending from mouth to ventral side of the exhalant aperture.

Labial palps: Absent.

Musculature: Adductor muscles present, isomyarian; with posterior and anterior pedal retractor muscles.

Foot: Small, short; pedal groove and byssal thread absent.

Digestive system: Funnel-shaped mouth opening into a thick and muscular oesophagus that enters into the anterodorsal portion of the stomach; oesophagus large with the presence of longitudinal internal grooves throughout its length; stomach rounded, large, probably dilated by the presence of large prey (maybe ostracods); stomach surrounded dorsally and anteriorly by the gonads and digestive gland and connected to the short and reduced crystalline style sac; crystalline style absent; presence of a thicker typhlosole between the style sac and proximal intestine; style sac conjoined with the midgut; pericardium/heart surround the rectum/hindgut and the kidney.

Organs of visceral mass: Haemocoel spaces observed close to the siphons.

Reproductive system: Hermaphroditic; ovary located dorsal to the visceral mass, closely associated to the

digestive gland; testis in the ventroposterior portion of visceral mass.

Nervous system: With observed circum-oesophagic, pedal and visceral ganglia.

Family Poromyidae Dall, 1886
Genus *Poromya* Forbes, 1844
Poromya rostrata Rehder, 1943
(Figs 10, 11)

Description

Shell: Ovate-trigonal, inflated, thin, whitish, inaequilateral, slightly inaequivalve; posterior margin with a short rostrum; outer sculpture granulated with micro-pustules over the entire shell; without lithodesma.

Mantle: Ventral mantle margin with one anteriorly wide pedal gape, extending from the anterior adductor until the inhalant siphon; without a fourth pallial aperture.

Siphons: Separated, different in size and outline; inhalant siphon, large, modified in a raptorial appendage, typically retracted into the infra-septal chamber; exhalant siphon short, cone-like and everted in this specimen; both surrounded at the base by a ring of large siphonal tentacles, 12 around the inhalant and three around exhalant; debris attached to the siphonal walls.

Septum: Thin, ventral surface with well-defined two-paired groups of slit-like branchial apertures, with no interfilamental connections; anterior group with four and posterior with five slits. Presence of a small and lobulate hollow sac in the posterior inner floor of the septum.

Labial palps: Non-lamellate, flattened and asymmetrical with anterior labial palps large and posterior labial palps small.

Musculature: Posterior and anterior adductor muscles present and isomyarian; with posterior and anterior pedal and septal retractor muscles; lateral septal muscles not visible in this specimen; taenioid muscle absent.

Foot: Large and elongated; absence of pedal groove and byssal thread.

Digestive system: The funnel-shaped mouth opens into a thick, short and muscular oesophagus that enters the anterodorsal portion of the stomach; with a sphincter between oesophagus and stomach opening; stomach large, rounded, internal grooves not visible into the gastric chamber; stomach connected to the short and small crystalline style sac located on the median portion of the stomach floor; no prey observed inside the stomach; stomach surrounded dorsally and anteriorly by the gonads and digestive gland; two gastric caeca observed in the digestive gland; crystalline style sac conjoined with the anterior portion of the midgut; crystalline style present; pericardium/heart surround the rectum/hindgut; hindgut passes above the kidney.

Reproductive system: Hermaphroditic, ovary and testis well visible; ovary closely associated to the digestive gland cover the roof and the posterior wall of the stomach; the testis lie ventral to the ovary and consist of a pair of large lobulate sacs.

Nervous system: With circum-oesophagic, pedal and visceral ganglia observed.

Family Cetoconchidae Dall, 1886
Genus *Cetoconcha* Forbes, 1844
Cetoconcha spinosula (Thiele, 1912) **comb. nov.**
(New combination for *Poromya spinosula* Thiele)
(Figs 12, 13)

Description

Shell: Ovate, relatively thick, inflated, equivalve and approximately equilateral; with a brownish periostracum and sand grains covering the shell; without lithodesma.

Mantle: Ventral mantle margin with one anterior and wide pedal gape, extending from the anterior adductor until two-thirds of the full length of ventral margin; posteroventral mantle margin fusion formed by inner folds (Type A) (Yonge, 1982); without a fourth pallial aperture.

Siphons: Separated, different in size and outline; inhalant siphon large, modified in a raptorial appendage, typically retracted into the infra-septal chamber when the living animal is at rest or, in museum specimens, due to the alcohol contraction; the inverted inhalant siphon can also be referred to in the literature as a siphonal cowl (hood) or branchial valve, the latter considered a misinterpretation (Pelseneer, 1911; Yonge 1928, Bernard, 1974, Morton, 1981); exhalant siphon short, cone-like; siphons surrounded at the base by a ring of large siphonal tentacles, ten around the inhalant and three around exhalant; presence of ~15 siphonal papillae between the siphonal tentacles.

Septum: Thin, transparent, perforated by three rows of grouped pores without interfilamental connections,

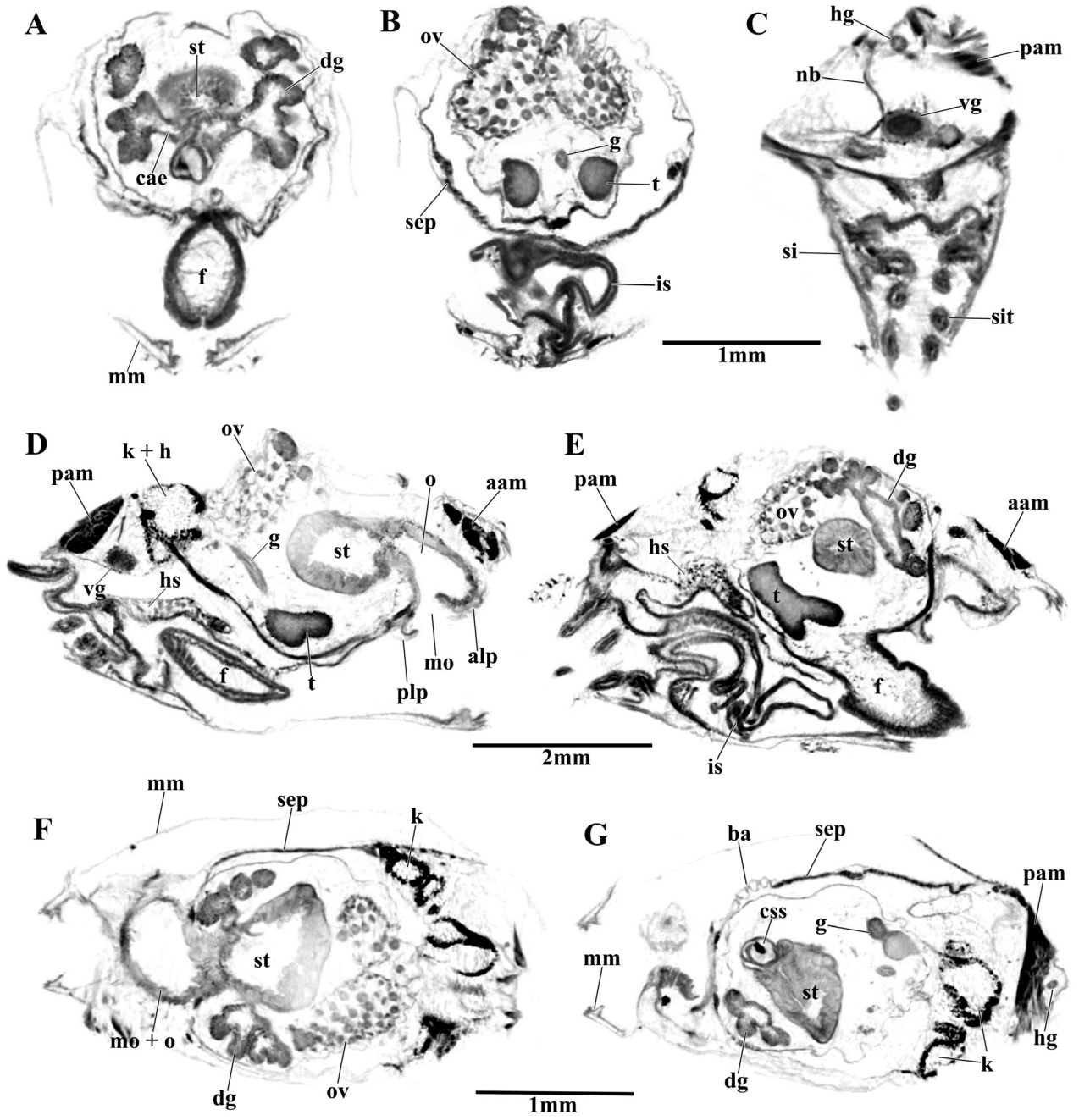

Figure 10. Selected virtual 2D sections through the micro-CT dataset of a PTA-stained specimen of *Poromya rostrata*. Transverse (A–C), sagittal (D, E) and frontal (F, G) sections. Scale bars: A–C, F, G = 1 mm; D, E = 2 mm.

comprising six pairs of pores anteriorly, five to six in the middle and four posteriorly. Presence of a swollen, hollow and bilobate sac in the posterior inner floor of the septum.

Labial palps: Non-lamellate and asymmetric with anterior labial palps well-developed, large, cup-shaped and posterior palps reduced, almost imperceptible in the 3D reconstructions.

Musculature: Posterior and anterior adductor muscles present, isomyarian; with posterior and anterior pedal and septal retractor muscles; lateral septal muscles and taenioid muscle absent.

Foot: Large and elongated; without pedal groove and byssal thread.

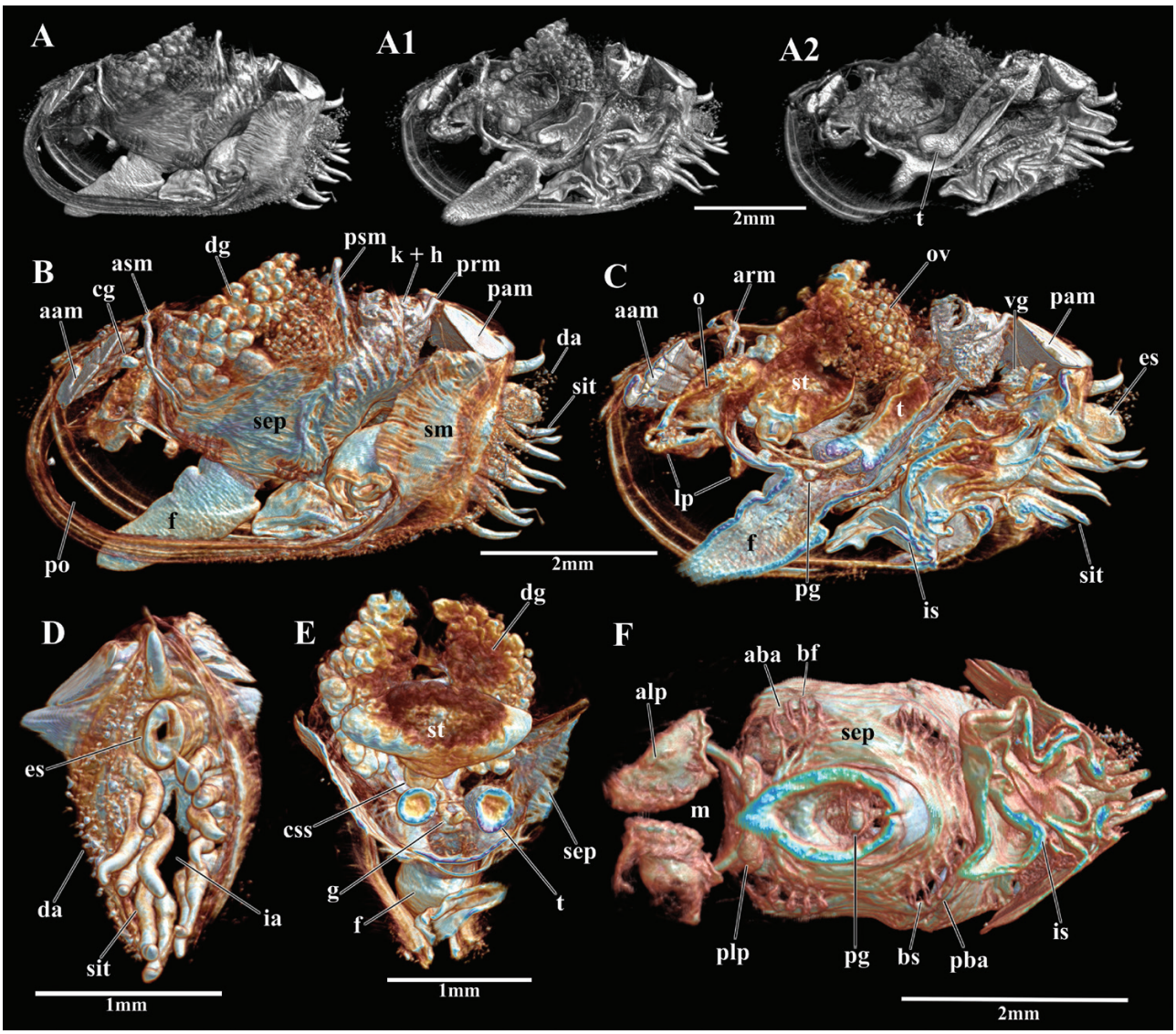

Figure 11. 3D volume rendering based on the micro-CT dataset of *Poromya rostrata*, displaying internal organs. Dissection sequence in original tomographic colour, lateral view (A–A2); false-colour volume rendering in lateral view (B) and virtual dissections in sagittal (C), transverse (D, E) and frontal (F) sections. Scale bars: A–C, F = 2 mm; D, E = 1 mm.

Digestive system: The funnel-shaped mouth opens into a thick, short and muscular oesophagus that enters the anterodorsal portion of the stomach; no sphincter was observed between oesophagus and stomach opening; stomach large, rounded, with longitudinal deep grooves in the posterodorsal and anteroventral walls; with prey inside the gastric chamber (maybe ostracod and copepods); stomach connected to the short and small crystalline style sac located at the ventroanterior portion of the stomach floor; stomach surrounded dorsally and anteriorly by the gonads and digestive gland; crystalline style sac conjoined with an anterior mid gut; crystalline style not visible; pericardium/heart surround the rectum/hindgut; hindgut passes above the kidney.

Organs of visceral mass: Haemocoel spaces present in the dorsoposterior portion of the visceral mass.

Reproductive system: Hermaphroditic; ovary and testis well visible, closely associated to the digestive gland; ovary dorsally located and testis in the anteroventral portion of the visceral mass, close to the lateral wall of the stomach.

Nervous system: Circum-oesophagic, pedal and visceral ganglia observed.

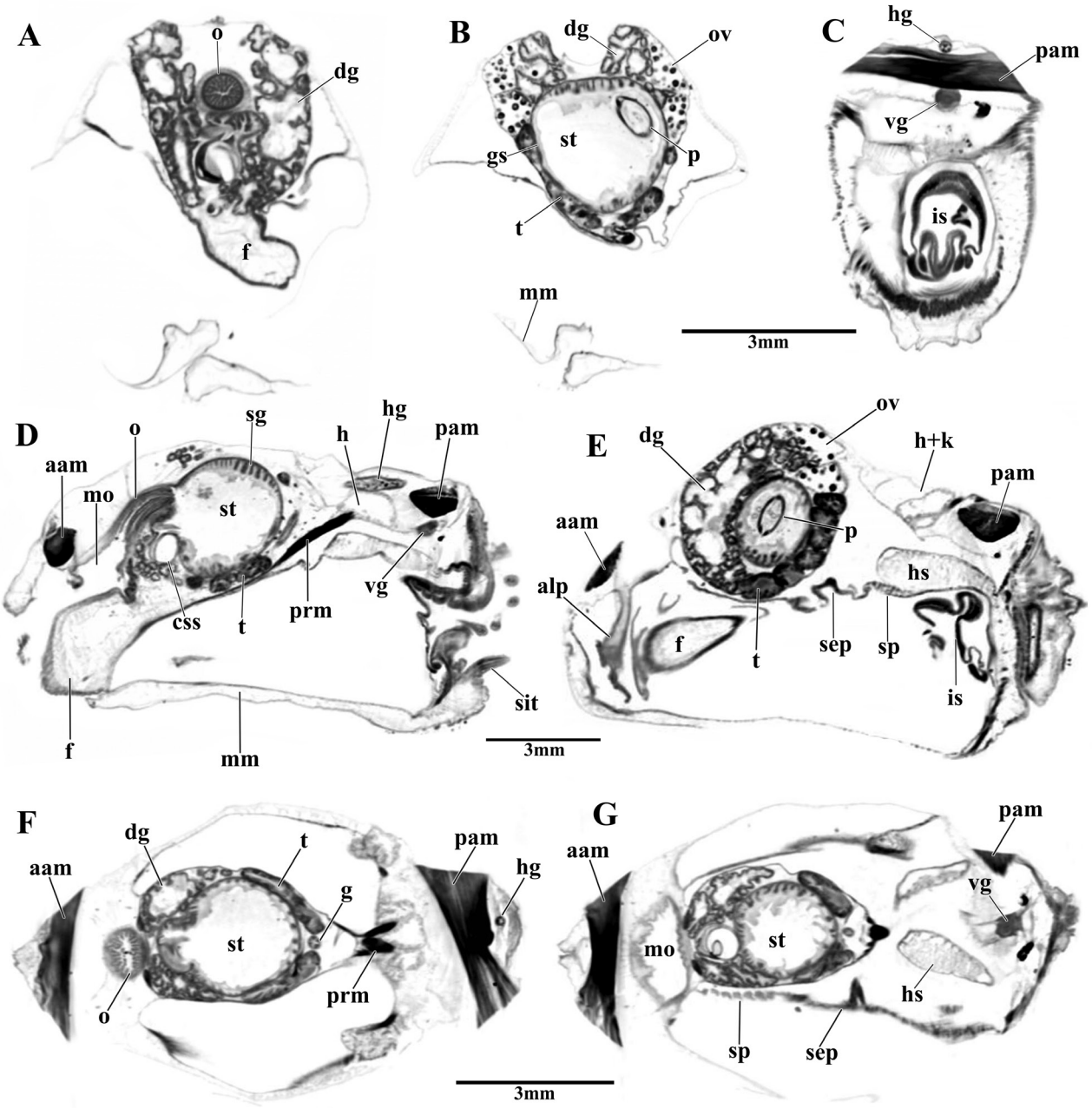

Figure 12. Selected virtual 2D sections through the micro-CT dataset of a PTA-stained specimen of *Cetoconcha spinosula* **comb. nov.** Transverse (A–C), sagittal (D, E) and frontal (F, G) sections. Scale bars: A–G = 3 mm.

FAMILY CETOCONCHIDAE RIDEWOOD, 1903

GENUS *CETOCONCHA* DALL, 1886

CETOCONCHA AFF. SMITHII (DALL, 1808)

(FIGS 14, 15)

Description

Shell: Ovate-trigonal, thin, inflated, slightly translucid, with prominent umbones, inflated; sculpture of radial lines of micro-pustules for the entire ventral surface of the valves; without lithodesma.

Mantle: Ventral mantle margin with one anteriorly wide pedal gape extending from the anterior adductor until the inhalant siphon; without a fourth pallial aperture.

Siphons: Separated, different in size and outline; inhalant siphon, large, modified in a raptorial appendage, typically retracted into the infra-septal chamber; exhalant siphon short, cone-like and everted in our specimen; both surrounded at the base by a ring of siphonal tentacles, ~ten around the inhalant and ~three around exhalant.

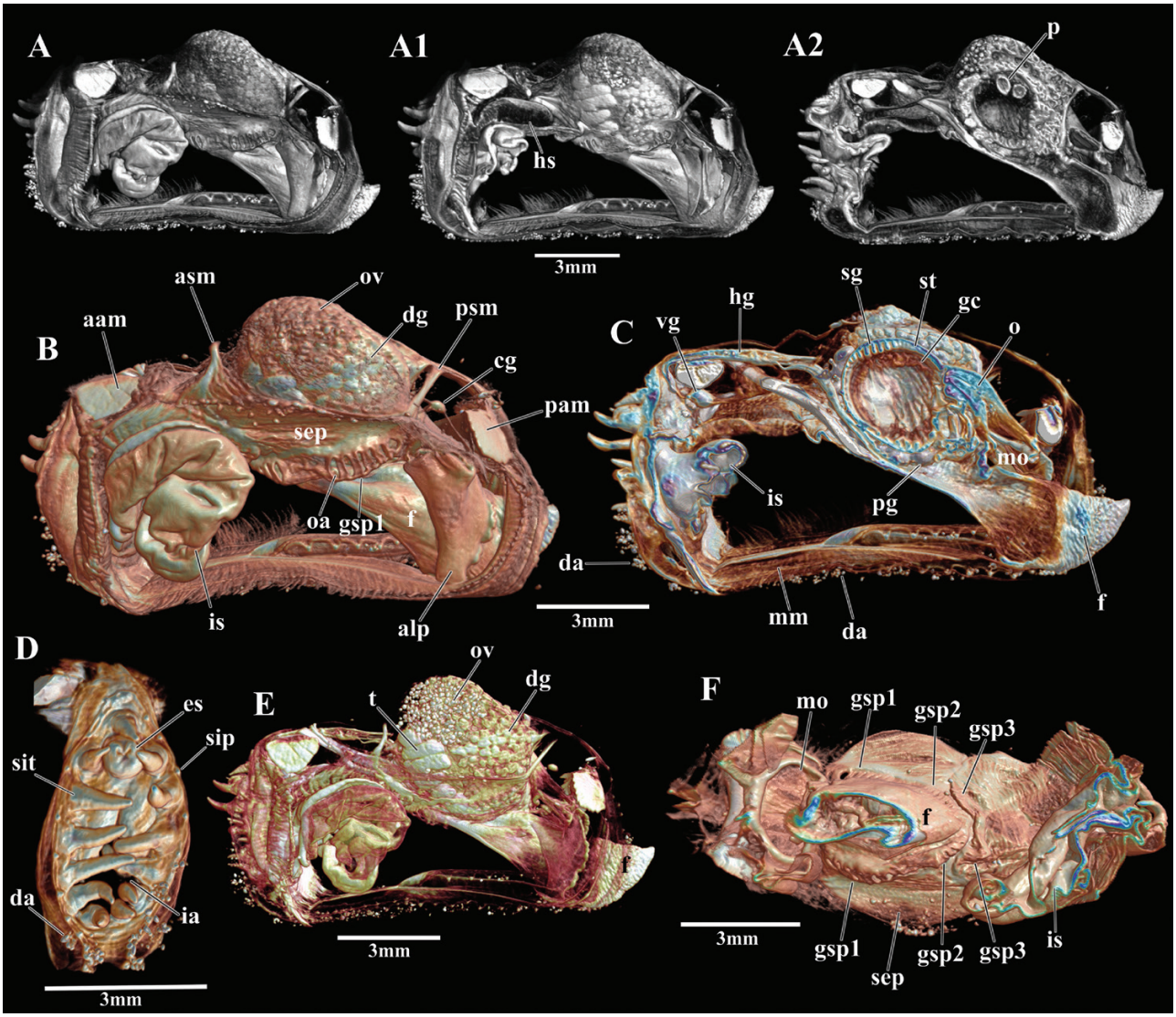

Figure 13. 3D volume rendering based on the micro-CT dataset of *Cetoconcha spinosula* **comb. nov.**, displaying internal organs. Dissection sequence in original tomographic colour, lateral view (A–A2); false-colour volume rendering, lateral view (B, E) and virtual dissections in sagittal (C), transverse (D) and frontal (F) sections. Scale bars: A–F = 3 mm.

Septum: Thin, perforated by three rows of grouped pores without interfilamental connections, the two anterior groups lie in a similar position to those of *Cetoconcha spinosula* **comb. nov.** and the third and smallest group lies behind the posterior septal muscles; bilobate hollow sac not observed in the posterior inner septal floor. With nine pairs of pores in the anterior group, five in the middle and three in the posterior group.

Labial palps: Non-lamellate and asymmetrical with anterior labial palps large, thin (probably contracted), cup-shaped and the posterior labial palps small.

Musculature: Posterior and anterior adductor muscles present and isomyarian; with posterior and anterior pedal and septal retractor muscles; prominent lateral septal muscles present; taenioid muscle absent.

Foot: Large, pedal groove not observed, without byssal thread.

Digestive system: The funnel-shaped mouth opens into a thick and muscular oesophagus that enters the anterodorsal portion of the stomach; stomach large, rounded, with longitudinal deep internal grooves in the dorsal wall, connected to the short and small crystalline style sac located in the median portion of the stomach floor; prey observed inside the stomach (ostracod: Fig. 14 A2); stomach surrounded dorsally and

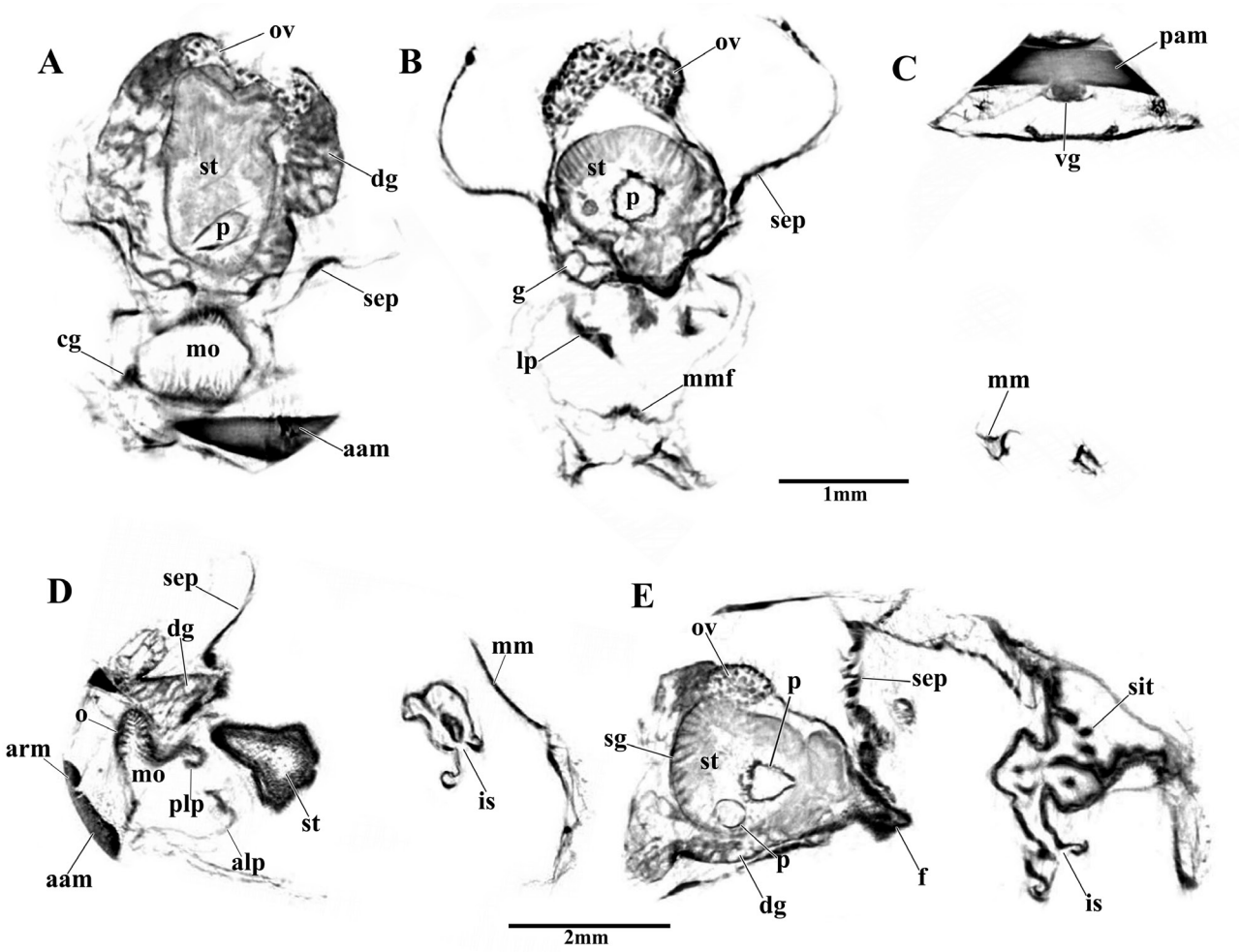

Figure 14. Selected virtual 2D sections through the micro-CT dataset of a PTA-stained specimen of *Cetoconcha* aff. *smithii*. Transverse (A–C), frontal slightly oblique (D, E) sections. Scale bars: A–C = 1 mm; D, E = 2 mm.

anteriorly by gonads and digestive gland; crystalline style sac not visible in this specimen.

Reproductive system: May be dioecious, only ovary is visible in our specimen; ovary closely associated to the digestive gland, covers the roof of the stomach.

Nervous system: only the visceral ganglia were observed.

FAMILY CUSPIDARIIDAE DALL, 1886

GENUS *CUSPIDARIA* NARDO, 1840

CUSPIDARIA GLACIALIS (SARS G. O., 1878)

(FIGS 16, 17)

Description

Shell: Elongated, robust, inaequilateral, equivalve and slightly inflated; with a prominent and long rostrum in the posterior; smooth, valves covered by a dehiscent, thick and light brown periostracum; with a lithodesma.

Mantle: Mantle margin with one anteriorly large pedal gape, extending from the anterior adductor until almost the beginning of the inhalant siphon; postero-ventral mantle margin fusion formed by inner and middle folds (Type B of Yonge, 1982); absence of a fourth pallial aperture.

Siphons: The detailed description of this structure was not possible due to the state of contraction of the specimen analysed.

Septum: Presence of a well-developed horizontal muscular septum ('septibranch condition') dividing the mantle cavity into infra- and supraseptal chambers; septum long and wide, perforated ventrally by five pairs of isolated septal pores.

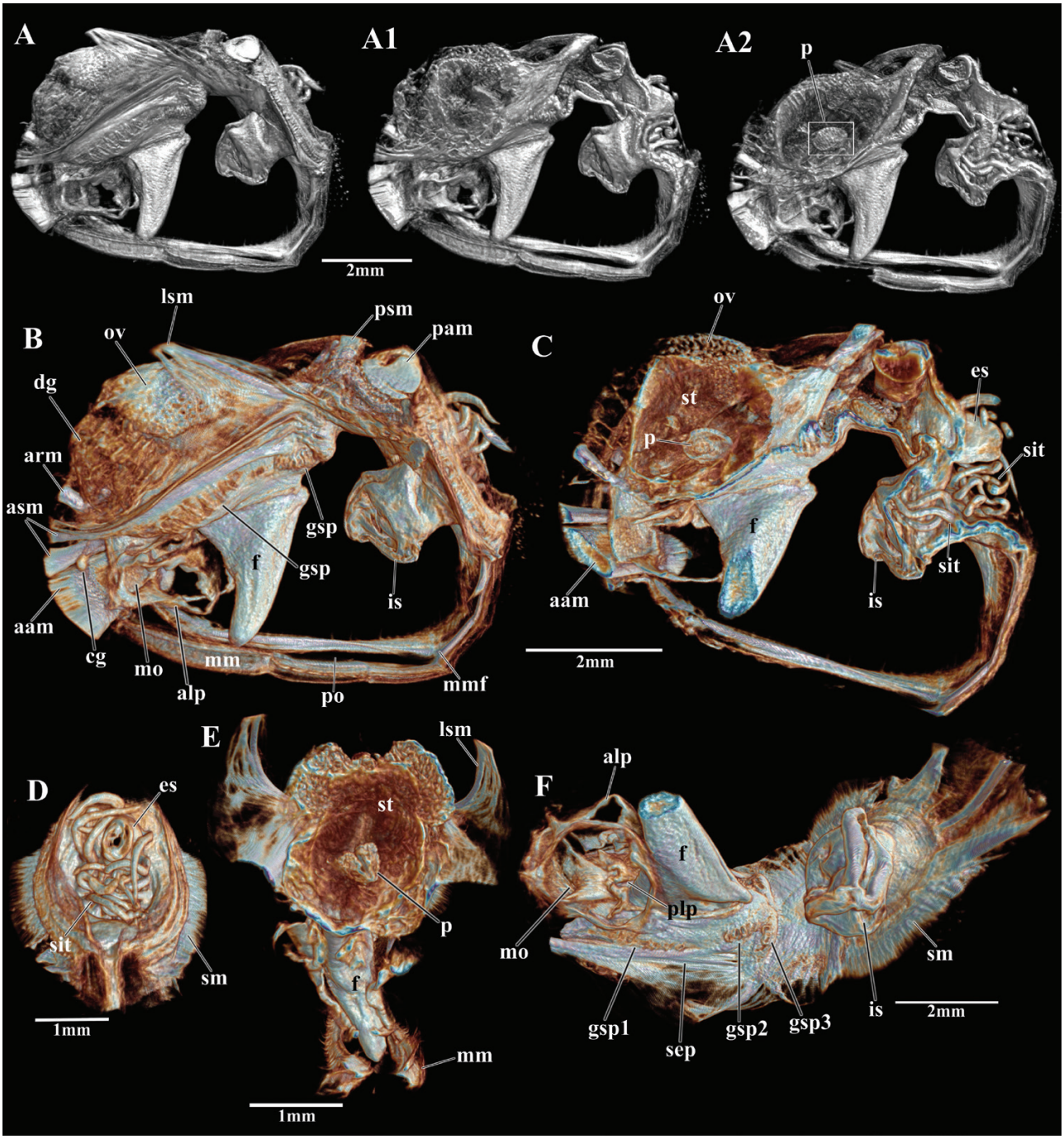

Figure 15. 3D volume rendering based on the micro-CT dataset of *Cetoconcha* aff. *smithii*, displaying internal organs. Dissection sequence in original tomographic colour, lateral view (A–A2); false-colour volume rendering, lateral view (B) and virtual dissections in sagittal (C), transverse (D, E) and frontal (F) sections. Scale bars: A–C, F = 2 mm; D, E = 1 mm.

Labial palps: Poorly developed, non-lamellate, slightly asymmetrical, with the anterior palps larger than the posteriors; anterior labial palps attached to ventroanterior mantle margin, close to anterior adductor muscle.

Musculature: Posterior and anterior adductor muscles present, isomyarian; with well-developed pedal and septal retractor muscles, both bifurcating before attaching to the shell; lateral septal muscle also present, more concentrated posteriorly; taenioid muscle absent.

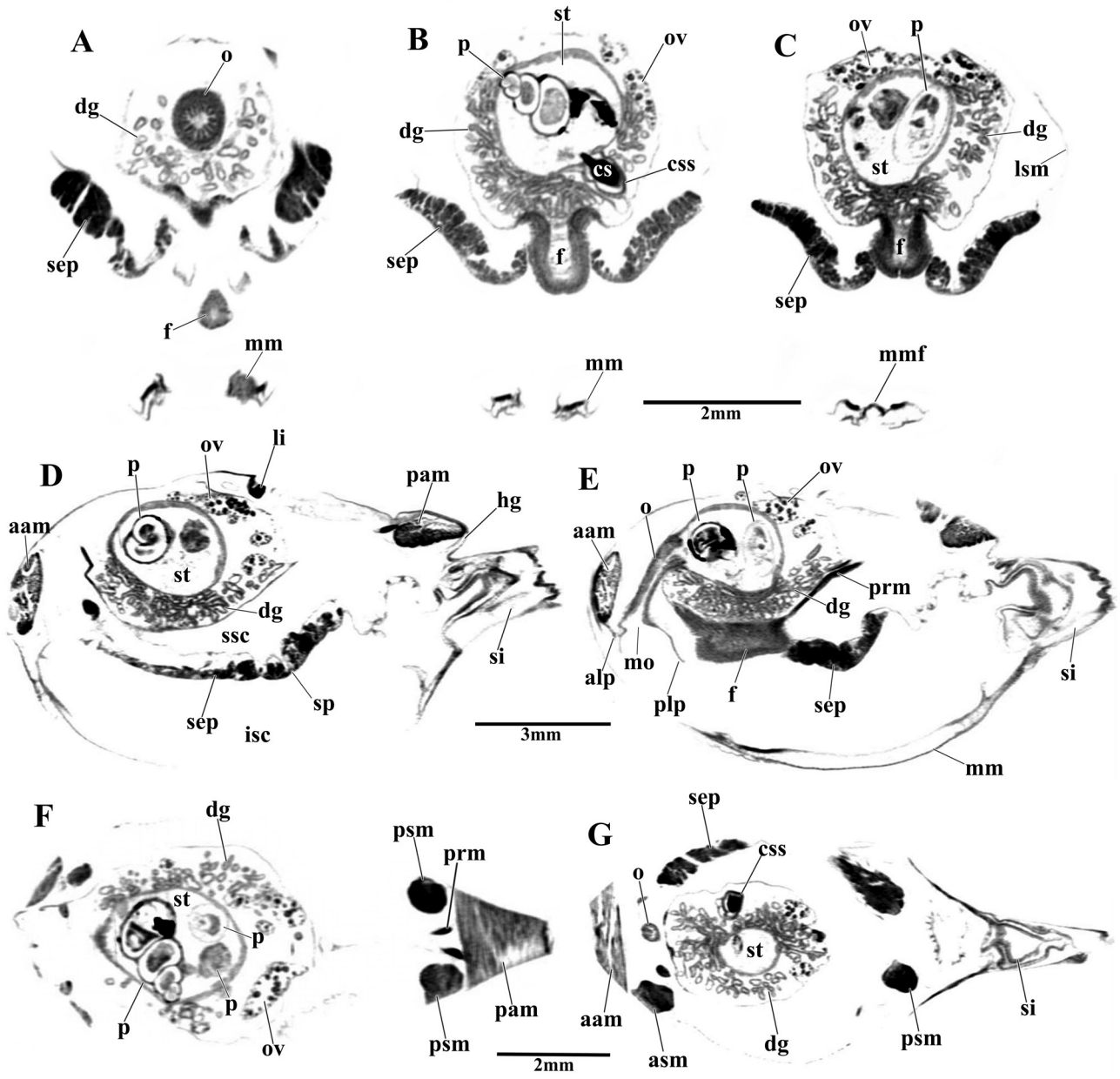

Figure 16. Selected virtual 2D sections through the micro-CT dataset of a PTA-stained specimen of *Cuspidaria glacialis*. Transverse (A–C), sagittal (D, E) and frontal (F, G) sections. Scale bars: A–C, F, G = 2 mm; D, E = 3 mm.

Foot: Large, with a long pedal groove; byssal thread absent.

Digestive system: Funnel-shaped mouth opens into thick and muscular oesophagus that enters into anterodorsal portion of stomach; stomach large, rounded, with a dorsal short projection, internal grooves not visible; stomach connected to the short and small crystalline style sac located on the median portion of the stomach floor; crystalline style present; large preys were observed inside of stomach (gastropod and ostracod: Figs 15B, F, 16D, E); stomach surrounded dorsally and anteriorly by the gonads and digestive gland.

Reproductive system: Dioecious, only ovary is visible in this specimen; ovary closely associated to the digestive gland, covering the roof of the stomach.

Nervous system: Only visceral ganglia observed.

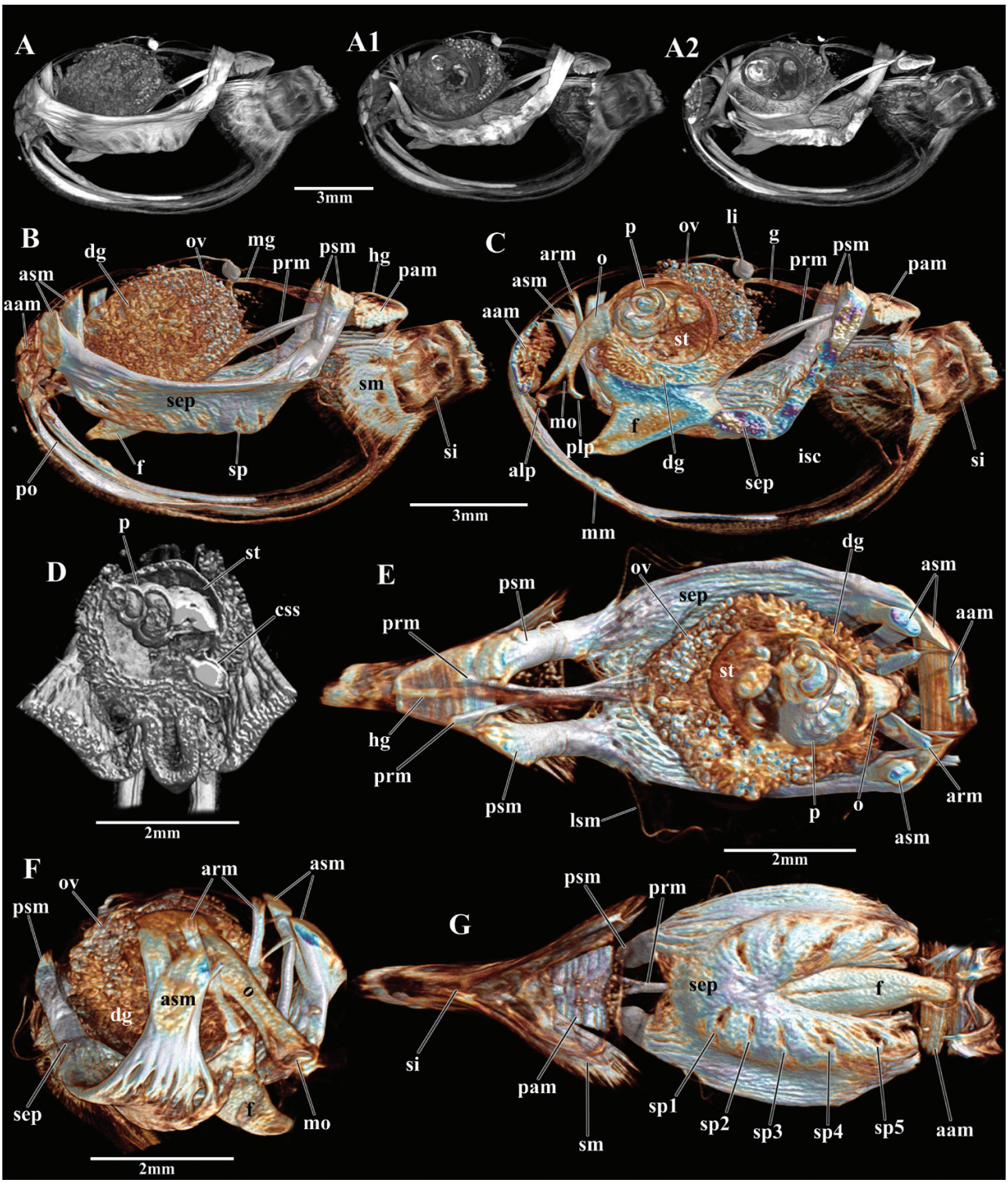

Figure 17. 3D volume rendering based on the micro-CT dataset of *Cuspidaria glacialis*, displaying internal organs. Dissection sequence in original tomographic colour, lateral view (A–A2); false-colour volume rendering, lateral view (B) and virtual dissections in sagittal (C), transverse (D, F) and frontal (E, G) sections. Scale bars: A–C = 3 mm; D–G = 2 mm.

DISCUSSION

Although some molluscan studies have already used micro-CT as a tool to obtain anatomical information (e.g. Golding & Jones, 2007; Golding *et al.*, 2009; Alba-Tercedor & Sánchez-Tocino, 2011; Faulwetter *et al.*, 2013b; Handschuh *et al.*, 2013; Candás *et al.*, 2016; Palmer *et al.*, 2017; Predouzo *et al.*, 2017), its application for bivalve systematics remains untested. The present study is, therefore, the first to comparatively evaluate the potential of this imaging technique for bivalve anatomy. Our results show that micro-CT is a useful tool for the anatomical description of bivalves, for individuals ranging in sizes from 3.2 to 13.8 mm in length, as well as for freshly fixed and for old museum specimens. We further show not only a detailed analysis of internal structures, but also a topographic visualization of the organs of the pallial cavity in 3D – in some cases with results comparable to those of dissections, histology and scientific illustrations. The 2D tomographic sections are also of extreme importance since they provide an interpretation at the histological level of organs of the visceral mass, as, for example, the alimentary tract path, the differentiation between male and female gonads, and nerve bundles, among others. Therefore, this minimally invasive technique proved to be efficient for describing the anatomy of marine bivalves, consequently being an important tool in the construction of the taxonomic and phylogenetic knowledge of Bivalvia.

A brief discussion of each internal anatomical feature considered of importance in anomalodesmatan taxonomy is provided below.

Mantle

The mantle margin of anomalodesmatans is extensively fused, presenting three main openings: a ventral and usually large pedal opening, and two posterior openings corresponding to the inhalant and exhalant siphons. Some anomalodesmatan species also present a fourth pallial opening, e.g. *Brechites attrahens* (Lightfoot, 1786), *Humphreyia strangei* (A. Adams, 1854) or *Lyonsia californica* Conrad, 1837, among others (Narchi, 1968: fig. 1; Morton, 1984b, 2002: fig. 8). This opening, located close to the base of the siphons, has been postulated to have a function related to facilitating the elimination of pseudofaeces from the pallial cavity, or could function as a pressure-release valve through which some of the mantle water is ejected following rapid adduction in fast-burrowing bivalves (Atkins, 1937; Yonge, 1952). Among the species analysed, only *Lyonsia alvarezii* presents a fourth pallial aperture. This aperture is also seen in representatives of a few non-anomalodesmatan imparidentian taxa, e.g. *Spisula*, *Lutraria* (Mactridae), *Ensis* (Pharidae), *Tagelus* (Solecurtidae) and *Siliqua* (Solenidae), but the homology between these structures has never been tested (Morton, 2010).

Mantle fusion in anomalodesmatans involves different mantle folds, and may be classified into types A, B or C, according to Yonge (1982). Through 2D tomographic sections we could observe the ventral fusion of the mantle in detail in a few species, as are the cases of *Allogramma formosa* (Fig. 6), *Trigonulina ornata* (Fig. 8) and *Cuspidaria glacialis* (Fig. 16), which have Type B; and *Cetoconcha spinosula* **comb. nov.** (Fig. 12), of Type A. It was not possible to observe the mantle fusion in the other species.

Musculature

The micro-CT reconstructions were very effective for the visualization of the muscular structures in the species analysed, allowing a topographical interpretation of the main muscles present in Anomalodesmata. Herein, the structure, position and insertion of the adductor muscles, foot retractors and septal muscles were described. Taenioid muscles were not observed in any of the species analysed. Usually associated to predatory bivalves, these muscles constitute a pair of hypertrophied muscular bundles inserted in the pallial sinus between the remaining siphonal retractor. In *Parilimya fragilis* (Grieg, 1920), for example, they serve to pull the inhalant siphon into the mantle cavity, assisting in prey capture (Morton, 1982). However, according to Morton (1984a: fig. 2), in *Allogramma formosa* (as *Lyonsiella formosa*) the taenioid muscle is modified and reduced to a few muscle bundles within the fused ventral mantle margin extending posteriorly into the inhalant siphon. Through a detailed analysis of the 2D tomographic sections, no muscle bundles were observed within the mantle margin or into the inhalant siphon of *Allogramma formosa*, confirming, therefore, the absence of a taenioid muscle in the specimen analysed.

For the species without a muscular septum, as *Pandora pinna*, *Lyonsia alvarezii*, *Trigonulina ornata* and *A. formosa*, adductor muscles with similar shape and size (isomyarian) and poorly developed pedal retractor muscles were observed, except for *Lyonsia alvarezii*, with a heteromyarian condition. The reduction of the pedal musculature is usually associated with the adoption of a passive burrowing or epifaunal lifestyle and had already been observed in other anomalodesmatans, including *Parilimya fragilis*, *Cleidothaerus albidus* (Lamarck, 1819) and in some clavagellids (Morton, 1974, 1982). Therefore, our results suggest that *Pandora pinna*, *Trigonulina ornata* and *A. formosa,* may also have a passive burrowing lifestyle. For *Lyonsia alvarezii*, specifically, the presence of a small byssal thread suggests an epifaunal lifestyle. In addition, the heteromyarian condition

observed in *Lyonsia alvarezii* seems to be a feature common to other lyonsiids, due to the effects of byssal attachment (see Yonge, 1952).

For the species that have a muscular septum, such as *Cetoconcha spinosula* **comb. nov.**, *Poromya rostrata*, *Cetoconcha* aff. *smithii* and *Cuspidaria glacialis*, the main differences are associated to the bifurcation of the retractor muscles of the foot and the septum, and the presence or absence of lateral septal muscles. These differences are mainly observed between some species of Poromyidae and Cetoconchidae, with the presence of a well-developed lateral septal musculature in *Cetoconcha* aff. *smithii* and absence in *Poromya rostrata*. In the same way, *Cuspidaria glacialis* (Cuspidariidae) has a muscular pattern that differs from those of poromyids and cetoconchids due to the presence of a thick and wide septum, presenting a well-developed and bifurcated posterior and anterior pedal and septal retractor muscles.

In general, the musculature of Anomalodesmata has not been used in taxonomic and phylogenetic studies of this group, although it is almost always described and sometimes well detailed (Allen & Turner, 1974; Allen & Morgan, 1981). Our results show that micro-CT can be useful in the rapid reconstruction and interpretation of muscular characters with a potential systematic significance.

Ctenidia

According to Harper *et al.* (2006) the anomalodesmatan ctenidia, when present, are complete, deeply plicate and heterorhabdic, defined as Type E of Atkins (1937). This type of eulamellibranch ctenidia is usually characterized by the presence of a complete inner demibranch and a reduced outer demibranch with only the descending lamellae. However, during the adaptive radiation of Anomalodesmata, ctenidia have been drastically reduced in the families Euciroidae, Lyonsiellidae and Verticordiidae, with remaining ctenidial filaments in Cetoconchidae and Poromyidae, or entirely lost in Cuspidariidae and Spheniopsidae (Allen & Morgan, 1974, 1981; Harper *et al.*, 2006; Morton *et al.*, 2016a, b). Among the species analysed, only *Pandora pinna* and *Lyonsia alvarezii* present a Type E ctenidia. In *Pandora pinna*, for example, the micro-CT images show a deep plicate ctenidia and a much reduced outer demibranch with the presence of a marginal food groove at the free edge of the inner demibranch. For *Lyonsia alvarezii*, the 3D reconstructions were important to visualize the disposition of demibranchs and a deep marginal groove. For both, the tomographic images were not able to show some gill details, e.g. the ctenidia filaments (shape, cilia) or the interfilamental junctions.

For *A. formosa* (Lyonsiellidae) and *Trigonulina ornata* (Verticordiidae) the micro-CT images showed a reduced ctenidia without a dorsal attachment with the visceral mass, giving it a horizontal orientation into the pallial cavity. According to Morton (1984a), the horizontal position of the ctenidia in *A. formosa* allows that the ctenidial axis separated posteriorly from the visceral mass divides the pallial cavity in supra- and infrabranchial chambers, a condition very similar to that observed in anomalodematans with a muscular septum. Still, for *A. formosa*, important details such as the ctenidial axis have been observed with the 2D tomographic sections.

The specimen of *Trigonulina ornata* scanned is the smallest among the species analysed, 3.2 mm in length. Notwithstanding, the 3D reconstructions were effective to visualize and consequently to understand the topography of the organs in the pallial cavity. The ctenidia of *Trigonulina ornata*, for example, are smaller and have fewer demibranch filaments than *A. formosa*, suggesting a morphological proximity with the septibranch condition. Although it is apparently closer, it is also worth noting that *Trigonulina ornata* have just the ctenidia, i.e. this species does not have any type of muscular septum associated with their gills. Other verticordiids as, for example, *Spinosipella deshayesiana* (P. Fischer, 1862) and *Spinosipella costeminens* (Poutiers, 1981) have ctenidia attached to a remaining septum (Simone & Cunha, 2008), showing an even greater proximity to the septal condition. Some molecular works also indicate a proximity between Verticordiidae and some septibranch species (Cuspidariidae, Poromyidae), although in all cases only one species of Verticordiidae has been used in the analyses, as *Verticordia* sp. in Dreyer *et al.* (2003) and Harper *et al.* (2006) or *Haliris tenerrima* (Thiele & Jaeckel, 1931) in Bieler *et al.* (2014) and Combosch *et al.* (2017); which may perhaps justify the low supports found by all of them.

The muscular septum and its associated musculature are some of the best-represented anatomical structures in our tomographic images, allowing for an excellent visualization of the different degrees of the ctenidial reduction. Therefore, it was also possible to distinguish thinner septa with remaining gill filaments (*Cetoconcha spinosula* **comb. nov.**, *Cetoconcha* aff. *smithii* and *Poromya rostrata*) from a thick and well-developed septum without ctenidial filaments (*Cuspidaria glacialis*). Furthermore, the 3D reconstructions facilitated the descriptions of the position and quantity of branchial apertures and septal pores present in these muscular septa, consequently, quickly providing key information for the taxonomy of the members of these families.

In general, Poromyidae includes species with a septum perforated by two paired groups of branchial apertures, being divided into two subfamilies, Poromyiinae, without interfilamental connections in the apertures

(usually slit-like or ostial apertures), and Cetomyinae, with such connections (usually sieve-like apertures) (Allen & Morgan, 1981; Krylova, 1997, 2001). The family Cetoconchidae, in turn, includes species with three paired groups of branchial apertures (grouped pores) represented by a single genus, *Cetoconcha*, presenting species with or without interfilamental connections, e.g. *Cetoconcha* (*Cribrosoconcha*) *alephtinae* and *Cetoconcha angolensis* Allen & Morgan, 1981, respectively (Allen & Morgan, 1981; Krylova, 1997, 2001). Based on this background, *Cetoconcha* aff. *smithii* and *Poromya rostrata* presented septal features corresponding to the diagnostic characteristics of their families, while the species previously identified as *Poromya spinosula* presents the characteristics of the genus *Cetoconcha*, since it has three ostial septal apertures (grouped pores). Therefore, we transfer *Poromya spinosula* Thiele, 1912 to *Cetoconcha* and Cetoconchidae, as *Cetoconcha spinosula* (Thiele, 1912) **comb. nov.**

Also associated with the septum, the presence of a bilobate hollow sac located in the posterior inner septal floor has been observed in *Cetoconcha spinosula* **comb. nov.** and *Poromya rostrata*. This structure is similar to the 'haemocoelic compensation sac' observed in *Poromya granulata* (Nyst & Westendorp, 1839) by Morton (1981). According to the latter author, this structure is associated with a complex mechanism of feeding and ingestion in *Poromya granulata* helping in the eversion of the inhalant siphon during prey capture through the release of fluids (Morton, 1981: fig. 15). Although not observed alive, the presence of this structure in *Cetoconcha spinosula* **comb. nov.** and *Poromya rostrata* suggests a similar prey capture mechanism to that described for *Poromya granulata*. This structure has not been observed in *Cetoconcha* aff. *smithii*, but this may be due to the contraction state of some organs of the posterior portion of the scanned specimen.

Finally, Cuspidariidae includes species with a thick and well-developed muscular septum (without ctenidial filaments) ventrally perforated by isolated pores. Usually presenting four pairs of pores, some genera can have different number of pores, as, for example, species of *Protocuspidaria* (5–30 pores) and *Halonympha* (8–20 pores) (Allen & Morgan, 1981; Krylova, 1994, 1995). The micro-CT reconstructions showed that *Cuspidaria glacialis* has a thick muscular septum perforated by five pairs of isolated pores. This number of pores is thus not common among species of *Cuspidaria* that usually present four pairs, although this same configuration has already been observed in *Cuspidaria cuspidata* by Allen & Morgan (1981: 453).

Labial palps

In general, the palps are considered important feeding structures in bivalves, since they assist the ctenidia in the conduction of the food particles available into the pallial cavity towards the mouth, to be ingested (Stasek, 1963). In Anomalodesmata the labial palps can be present or absent, large or reduced, symmetrical or asymmetrical, lamellate with sorting ridges in the filter-feeding species (typical bivalve anatomy) or non-lamellate and usually modified in the carnivorous species. Herein, the 3D reconstructions provided good-quality images for the main characteristics of this structure and when present, anterior and posterior labial palps were described.

Among the species scanned, *Trigonulina ornata* is the only one that does not have labial palps. The suspension-feeders *Pandora pinna* and *Lyonsia alvarezii* have large, lamellate and symmetrical labial palps while the other five carnivorous species have non-lamellate and modified outer and inner palps (asymmetrical). The absence of labial palps is rare among anomalodesmatans and appears to be exclusively associated with minute-sized carnivorous species, such as *Trigonulina ornata* and the spheniopsids *Grippina coronata* Machado & Passos, 2015 (1.67 mm in length) and *Spheniopsis brasiliensis* Machado & Passos, 2015 (1.78 mm in length) (Machado & Passos, 2015; Morton *et al*., 2016a, b). According to Morton *et al.* (2016b), in species without labial palps, the foot is probably used to push inhaled prey from the infra-septal chamber towards the mouth.

For the carnivorous species, *Cetoconcha spinosula* **comb. nov.**, *Poromya rostrata* and *Cetoconcha* aff. *smithii*, the anterior labial palps are larger than the posterior; *A. formosa* has extremely complex labial palps, while *Cuspidaria glacialis* possesses reduced labial palps. In species of Poromyiidae and Cetoconchidae, for example, the palp pattern observed (anterior larger and posterior reduced) has been also reported for most species of these families, including *Poromya australis* E. A. Smith, 1885, *Cetomya tornata* (Jeffreys, 1876), *Lissomya rotundula* Krylova, 1997 and *Cetoconcha angolensis* among others (Allen & Morgan, 1981; Krylova, 1997, 2001), being, therefore, an important characteristic for the systematics of this group.

The palps of *A. formosa* are complex, fused medially forming two globular flask-shaped buccal cavities below the mouth, very similar to the palp descriptions made by Morton (1984a) and Allen & Turner (1974) for the species *A. formosa*. The function for these fused palps is unknown; however, the unfused part (fluted funnels) probably assists the inhalant siphon in driving the prey toward the mouth.

For Cuspidariidae, the labial palps are generally small and reduced, and can be classified as Type I, II and III (see Allen & Morgan, 1981: 438–439). The reduced palps of *Cuspidaria glacialis*, specifically, also follow the same cuspidariid pattern, being similar to the palps observed

for other *Cuspidaria* species and, therefore, classified as Type II by Allen & Morgan (1981).

Siphons

The siphons are muscular structures formed by the mantle margin fusion that perform the function of connecting the internal bivalve structures to the environment around them, allowing for exploring food resources, conducting gas exchange and releasing gametes. In Anomalodesmata, the siphons can be fused or separated, similar or different in size and outline, encased or not in a periostracal or in a tissue sheath, with or without sensorial tentacles; the inhalant siphon can be a simple tube or highly modified, among other characters. Important for the taxonomy of Anomalodesmata, the siphons are also structures widely used in phylogenetic studies, presenting a strong phylogenetic signal (e.g. Harper *et al.*, 2000; Giribet & Wheeler, 2002; Bieler *et al.*, 2014).

The micro-CT images, mainly 3D reconstructions, were very effective for visualizing the inhalant and exhalant siphons, siphonal apertures, associated musculature and the number and position of sensory tentacles, allowing for an accurate description of these structures. Except for *Cuspidaria glacialis*, all species had their siphons and sensorial tentacles characterized. *Pandora pinna* and *Lyonsia alvarezii* were the only species to present siphons with the same size and outline (suspension-feeders), *Trigonulina ornata* has a short and half cone-shaped inhalant and a non-visible exhalant siphon, and for the other species the inhalant siphon was modified into a raptorial structure usually associated with prey capture (predatory bivalves).

The raptorial inhalant siphons of *A. formosa*, *Cetoconcha spinosula* **comb. nov.**, *Poromya rostrata* and *Cetoconcha* aff. *smithii* are similar in size and outline, being usually visualized inverted into the pallial cavity. For these species, sensorial tentacles are always present at the base of the siphons, usually presenting variation in terms of shape, quantity and position. In *A. formosa*, for example, two different types of siphonal tentacles were identified, ~50 smaller tentacles resembling papillae located closest to the siphonal apertures and ~60 larger tentacles, with a finger-like shape, peripherally located. According to Morton (1984a), the siphons of *A. formosa* are surrounded by a ring of ~48 tentacles arranged in two cycles; those of the outer cycle are larger and longer than those of the inner; results partially similar to those observed via 3D reconstructions, except for the number of tentacles.

For Poromyidae, specifically, the arrangement (number and position of siphonal tentacles and papillae) is important for the taxonomy of this group (Krylova, 2001: fig. 17). Herein, the species *Poromya rostrata* (12 is, 3es + 0 sip) presents a configuration similar to that reported for *Poromya undosa* Hedley & Petterd, 1906 (10 is, 3es + 0 sip) but different to that of *Cetomya poutiersi* Krylova, 2001 (10 is, 3 es + 12 sip) and *Cetomya celsa* Krylova, 2001 (10 is, 3 es + 10 sip), indicating the potential of these siphonal arrangements for differentiation at the genus level.

The arrangement described for the cetoconchid *Cetoconcha spinosula* **comb. nov.** (10 is, 3es + 15 sip) is different to that observed in *Cetoconcha* aff. *smithii* (10 is, 3 es + 0 sip), mainly due to the absence of siphonal papillae (sip) in the latter. On the other hand, the siphonal configuration of *Cetoconcha* aff. *smithii* is similar to that reported for *Cetoconcha angolensis* and *Cetoconcha braziliensis* by Allen & Morgan (1981), i.e. 15 tentacles around the siphons and no papillae. This paper shows for the first time the presence of siphonal papillae for a member of Cetoconchidae, indicating, therefore, a possible similarity between the siphonal arrangement of *Cetoconcha spinosula* **comb. nov.** and some poromyid members. While molecular data are available for Poromyidae, no data have been published on Cetoconchidae (Combosch *et al.*, 2017), but it would be interesting to see whether these families are supported molecularly.

Alimentary tract

Among the main structures that compose the digestive system, the stomach is one of the most complex and character-rich organs in bivalves, since the gastric chamber morphology provides multiple characters (Bieler *et al.*, 2014). For Anomalodesmata, specifically, two different types of stomach are reported, Type II and Type IV (Purchon, 1956, 1987). In general, the morphology of the stomach Type II is associated with the carnivorous habit characterized by a large rounded sac with thick muscular walls and extensive scleroprotein linings, which facilitate crushing prey; the stomach is combined with a reduced crystalline style sac (short crystalline style) plus a muscular oesophagus and a large mouth. Associated with filter-feeder anomalodesmatans, the Type IV comprises a small and oval stomach associated with an elongated and non-muscularized oesophagus and a small mouth, and a gastric chamber elongated ventrally, combined with the crystalline style sac and the presence of numerous gastric caeca (Purchon, 1956, 1987; Harper *et al.*, 2006; Mikkelsen & Bieler, 2008).

The micro-CT images showed with a good quality most of these structures, allowing for the classification of the stomach type for the species analysed. Therefore, *Trigonulina ornata*, *Cetoconcha spinosula* **comb. nov.**, *Poromya rostrata*, *Cuspidaria glacialis* and *Cetoconcha* aff. *smithii* have a Type II stomach, while *Pandora pinna* and *Lyonsia alvarezii* have a Type IV.

Allogramma formosa is the only species belonging to a traditionally carnivorous family (Lyonsiellidae) that presents an intermediate morphology between Types II and IV, with a small and oval stomach associated with a well-developed muscular oesophagus. Although uncommon among bivalves, the carnivorous species *Parilimya fragilis* (Parilimyidae) and *Propeamussium jeffreysii* (E. A. Smith, 1885) (Propeamussiidae) also display an intermediate morphology between that of a filter-feeder and that of a more specialized carnivore (Purchon, 1987, 1990; Tëmkin & Strong, 2013). It is worth noting that *A. formosa* also has a well-developed sphincter between the oesophagus and the stomach (oesophageal opening), very similar to the muscular sphincter reported for *Bathyneaera demistriata* (Allen & Morgan, 1981) (Cuspidariidae) by Tëmkin & Strong (2013).

In addition, most Type II species have whole prey inside the stomach, demonstrating their carnivorous habits. The tomographic images also show a gastropod inside the stomach of *Cuspidaria glacialis*, a type of prey never before reported for a cuspidariid (Morton 1987: table 1). Gastropods had already been found in the stomach of some poromyiids, e.g. *Cetomya butoni* (Prashad, 1932), *Cetomya bacata* Krylova, 2001 and *Cetomya celsa* Krylova, 2001 (Krylova, 2001: table 1).

Other structures related to the alimentary system and difficult to observe with other methods, including the path of the gut, details about the midgut, the relationship between hindgut (rectum), kidney and heart were also visualized through the 2D tomographic images for all species scanned.

Using tomographic data in phylogenetic reconstructions

The acquisition of high-quality tomographic data for the morphological study of marine invertebrates is relatively recent (e.g. Faulwetter *et al.*, 2013a; Candás *et al.*, 2014, 2016, 2017) and important questions related to specimen preparation, contrast solutions, image processing, 3D reconstructions, effect of radiation on DNA structure and dissemination of data, are still being debated (Faulwetter *et al.*, 2014). The expansion in the use of micro-CT has shown the great potential of this tool for the taxonomy of specific groups, generating morphological data that could be used for phylogenetic analyses (Faulwetter *et al.*, 2013b; Parapar *et al.*, 2017).

For molluscs, the effectiveness of micro-CT for the study of anatomy has been tested extensively (Golding & Jones, 2007; Golding *et al.*, 2009; Alba-Tercedor & Sánchez-Tocino, 2011; Malkowsky & Jochum, 2014; Candás *et al.*, 2016; Predouzo *et al.*, 2017), but few studies have focused on systematics or comparative approaches. The present study, therefore, is the first to present detailed anatomical data obtained exclusively via micro-CT showing potential for rapid anatomical study. The tomographic datasets acquired (2D/3D) for the anomalodesmatan species allow easy access to internal features (virtual dissections) and can assist in the identification of species, anatomical comparisons and coding of morphological characters.

Compared to more traditional techniques (dissection, SEM, TEM, histology), micro-CT is faster and minimally invasive, allowing the study of small and rare specimens, as exemplified in this paper. However, limitations inherent to micro-CT scanners, including the ability to distinguish organs of similar density and lack of resolution during the reconstructions of small structures (<80 µm), still render importance to traditional techniques. For anomalodesmatans, these limitations would include the study of shell microstructure (microstructural arrangements, layers of myostracum, intraperiostracal calcification), sperm ultrastructure and statocysts (see Bieler *et al.*, 2014, chars. 29–38, 45, 192–210; Harper *et al.*, 2000, char. 37), which would require the use of scanning and transmission electron microscopy.

Despite these limitations, an advantage of micro-CT is the ability to examine organs in their natural position, allowing for better understanding of functional morphology and homology or for the discovery of new diagnostic characters (Faulwetter *et al.*, 2014). This resource was fundamental to relate structures such as the 'bilobate hollow sac' in *Cetoconcha spinosula* **comb. nov.** and *Poromya rostrata* with 'haemocoelic compensation sac' described for *Poromya granulata*; and the arrangement of the siphonal tentacles, morphology of the labial palps and number of septal apertures in members of Cuspidariidae, Lyonsiellidae, Poromyidae and Cetoconchidae.

Although there are pros and cons in relation to micro-CT, the resolution power of invasive tools (histology, SEM, TEM and dissections) is indisputable and remains important for the acquisition of morphological data of minute bivalves. Therefore, the use of micro-CT in combination with traditional techniques could bring significant advances for the understanding of Bivalvia.

CONCLUSIONS

Our results demonstrate that X-ray micro-CT is a tool with great potential for the relatively rapid study of the anatomy of small bivalves. Micro-CT proved to be a fast and precise tool, resulting in 3D reconstructions and 2D tomographic sections of high quality. This study provides tomographic anatomical data for eight anomalodesmatan species, *Pandora pinna*, *Lyonsia alvarezii*, *Trigonulina ornata*, *A. formosa*, *Cetoconcha spinosula* **comb. nov.**, *Poromya rostrata*, *Cetoconcha*

aff. *smithii* and *Cuspidaria glacialis*; discusses some characters of *A. formosa* and transfers *Poromya spinosula* Thiele, 1912 to the genus *Cetoconcha*. Although the micro-CT scanners used in this study present resolution limitations, especially for structures <80 µm, new instrument development, including nano-CT and True-colour micro-CT are becoming more accessible and will allow increases in the resolution and sharpness of the tomographic images, consequently making of this technique a potential tool for the development of a new taxonomic era of high-throughput anatomical data (see Ziegler & Menze, 2013).

ACKNOWLEDGEMENTS

We acknowledge the support of the Department of Organismic & Evolutionary Biology (OEB-Harvard University) and Brazilian Nanotechnology National Laboratory (LNNano- CNPEM) during the use of the scanners facilities. We are also grateful to the the Museu de Zoologia da Universidade Estadual de Campinas 'Adão José Cardoso' (ZUEC) for the loan of material and to the staff of the Museum of Comparative Zoology – Harvard University (MCZ) for assisting with specimens. Special thanks go to Adam Baldinger, Murat Recevik (MCZ) and Dr Michela Borges (ZUEC) for kindly helping the first author with specimens. Jennifer W. Trimble (MCZ) is acknowledged for providing initial training on the micro-CT 1173 and Bruna P. Massucato and Rubia F. Gouveia (LNNano/CNPEM) for their help during the image acquisition in the micro-CT 1272. Special thanks due to Dr Guido Pastorino (Museo Argentino de Ciencias Naturales 'Bernardino Rivadavia') for the specimens of *A. formosa* and *Cetoconcha spinosula* from Argentina, and due to Dr Alexander Ziegler (Institut für Evolutionsbiologie und Ökologie, Bonn University) for exchanging ideas with FMM about tomographic techniques. We also would like to thank the Editor, Dr Liz Harper and an anonymous reviewer for their suggestions, which helped to improve this manuscript. Financial support was provided by a regular and PhD. sandwich (No. 88881.131768/2016-01) scholarships from CAPES to F.M.M and from internal funds of the MCZ.

REFERENCES

Alba-Tercedor J, Sánchez-Tocino L. 2011. The use of the SkyScan 1172 high resolution micro-CT to elucidate if the spicules of the sea slugs (Mollusca: Nudibranchia, Opisthobranchia) have a structural or a defensive function. *SkyScan Users Meeting* 113–121.

Allen JA. 1954. On the structure and adaptations of *Pandora inaequivalvis* and *P. pinna*. *Quarterly Journal of Microscopical Science* **95:** 473–482.

Allen JA. 2008. Bivalvia of the deep Atlantic. *Malacologia* **50:** 57–173.

Allen JA, Morgan ER. 1981. The functional morphology of Atlantic deep water species of the families Cuspidariidae and Poromyidae (Bivalvia): An analysis of the evolution of the septibranch condition. *Philosophical Transactions of the Royal Society of London, Series B: Biological Sciences* **294:** 413–546.

Allen JA, Turner JF. 1974. On the functional morphology of the family Verticortiidae (Bivalvia) with descriptions of new species from the abyssal Atlantic. *Philosophical Transactions of the Royal Society of London* **268:** 401–536.

Atkins D. 1937. On the ciliary mechanisms and interrelationships of lamellibranchs. Part III: types of lamellibranch gills and their food currents. *Quarterly Journal of Microscopical Research* **79:** 375–421.

Bernard FR. 1974. Septibranchs of the eastern Pacific (Bivalvia: Anomalodesmata). *Allan Hancock Monographs in Marine Biology* **8:** 1–279.

Bieler R, Mikkelsen PM, Collins TM, Glover EA, González VL, Graf DL, Harper EH, Healy J, Kawauchi GY, Sharma PP, Staubach S, Strong EE, John JD, Tëmkin I, Zardus JD, Clark S, Guzmán A, McIntyre E, Sharp P, Giribet G. 2014. Investigating the Bivalve Tree of Life – an exemplar-based approach combining molecular and novel morphological characters. *Invertebrate Systematics* **28:** 32–115.

Bieler R, Mikkelsen PM, Gonzalo G. 2013. Bivalvia – a discussion of known unknowns. *American Malacological Bulletin* **31:**123–133.

Candás M, Díaz-Agras G, Abad M, Baniol L, Cunha-Veira X, Pedrouzo L, Señaris MP, Tato R, García-Álvarez Ó, Urgorri V. 2016. Application of micro-CT in the study of the anatomy of small marine molluscs. *Microscopy and Analysis* **30:** S8–S11.

Candás M, Díaz-Agras G, Urgorri V. 2014. The use of micro-CT for the study of the internal anatomy of sea slugs (Opisthobranchia, Nudibranchia, Dotidae). *SkyScan Users Meeting* 241–243.

Candás M, Díaz-Agras G, Urgorri V. 2017. First steps in morphological analysis of the of the reproductive system of *Doto pinnatifida* (Montagu,1804). *Micro-CT User Meeting* 112–116.

Carbayo F, Francoy TM, Giribet G. 2016. Non-destructive imaging to describe a new species of *Obama* land planarian (Platyhelminthes, Tricladida). *Zoologica Scripta* **45:** 566–578.

Combosch DJ, Collins TM, Glover EA, Graf DL, Harper EM, Healy JM, Kawauchi GY, Lemer S, McIntyre E, Strong EE, Taylor JD, Zardus JD, Mikkelsen PM, Giribet G, Bieler R. 2017. A family-level tree of life for bivalves based on a Sanger-sequencing approach. *Molecular Phylogenetics and Evolution* **107:** 191–208.

Cox LR. 1969. *General features of the Bivalvia*. In: Moore R, Lawrence KS, eds. *Treatise on invertebrate paleontology, Part I, Mollusca 1*. University of Kansas Press and Geological Society of America, N2–N129.

Dreyer H, Steiner G, Harper EM. 2003. Molecular phylogeny of Anomalodesmata (Mollusca: Bivalvia) inferred from 18S rRNA sequences. *Zoological Journal of the Linnean Society* **139:** 229–246.

Faulwetter S, Dailianis T, Vasileiadou A, Arvanitidis C. 2013a. Contrast enhancing techniques for the application of micro-CT in marine biodiversity studies. *Microscopy and Analysis* **27:** S4–S7.

Faulwetter S, Dailianis T, Vasileiadou K, Kouratoras M, Arvanitidis C. 2014. Can micro-CT become an essential tool for the 21st century taxonomist? An evaluation using marine polychaetes. *Microscopy and Analysis* **28:** S9–S11.

Faulwetter S, Vasileiadou A, Kouratoras M, Dailianis T, Arvanitidis C. 2013b. Micro-computed tomography: introducing new dimensions to taxonomy. *ZooKeys* **263:** 1–45.

Fernández R, Kvist S, Lenihan J, Giribet G, Ziegler A. 2014. *Sine systemate chaos*? A versatile tool for earthworm taxonomy: non-destructive imaging of freshly fixed and museum specimens using micro-computed tomography. *PLoS One* **9:** e96617.

Giribet G. 2008. *Bivalvia*. In: Ponder WF, Lindberg DR, eds. *Phylogeny and evolution of the Mollusca*. Berkeley, CA: University of California Press, 105–141.

Giribet G, Wheeler W. 2002. On bivalve phylogeny: a high-level analysis of the Bivalvia (Mollusca) based on combined morphology and DNA sequence data. *Invertebrate Biology* **121:** 271–324.

Gofas S. 2017. *Bivalvia*. Accessed through: World Register of Marine Species at http://www.marinespecies.org/aphia.php?p=taxdetails&id=105 on 2017-11-28 (accessed 10 June 2018).

Golding RE, Jones AS. 2007. Micro-CT as a novel technique for 3D reconstruction of molluscan anatomy. *Molluscan Research* **27:** 123–128.

Golding RE, Ponder WF, Byrne M. 2009. Three-dimensional reconstruction of the odontophoral cartilages of Caenogastropoda (Mollusca: Gastropoda) using micro-CT: morphology and phylogenetic significance. *Journal of Morphology* **270:** 558–587.

Handschuh S, Baeumler N, Schwaha T, Ruthensteiner B. 2013. A correlative approach for combining microCT, light and transmission electron microscopy in a single 3D scenario. *Frontiers in Zoology* **10:** 44.

Harper EM, Dreyer H, Steiner G. 2006. Reconstructing the Anomalodesmata (Mollusca: Bivalvia): morphology and molecules. *Zoological Journal of the Linnean Society* **148:** 395–420.

Harper EM, Hide EA, Morton B. 2000. Relationships between the extant Anomalodesmata: a cladistic test. In: Harper EM, Crame JA, Taylor JD, eds. *The evolutionary biology of the Bivalvia. The Geological Society of London* **177:** 129–143.

Healy JM, Bieler R, Mikkelsen PM. 2008. Spermatozoa of the Anomalodesmata (Bivalvia, Mollusca) with special reference to relationships within the group. *Acta Zoologica (Stockholm)* **89:** 339–350.

Kerbl A, Handschuh S, Nödl M-T, Metscher B, Walzl M, Wanninger A. 2013. Micro-CT in cephalopod research: Investigating the internal anatomy of a sepiolid squid using a non-destructive technique with special focus on the ganglionic system. *Journal of Experimental Marine Biology and Ecology* **447:** 140–148.

Knudsen J. 1970. The systematics and biology of abyssal and hadal Bivalvia. *Galathea Reports* **11:** 1–241.

Krylova EM. 1991. A new genus and two new species of bivalve molluscs of the family Cetoconchidae (Bivalvia, Septibranchia, Poromyoidea). *Zoologicheskyi Zhurnal* **70:** 132–136.

Krylova EM. 1994. Clams of the genus *Octoporia* (Septibranchia: Halonymphidae) in the world oceans. *Zoologicheskyi Zhurnal* **73:** 38–45 [in Russian].

Krylova EM. 1995. Clams of the family Protocuspidariidae (Septibranchia, Cuspidarioidea): taxonomy and distribution. *Zoologicheskii Zhurnal* **74:** 20–38 [in Russian].

Krylova EM. 1997. New taxa and the system of the recent representatives of the family Poromyidae (Bivalvia, Septibranchia, Poromyoidea). *Ruthenica* **7:** 141–148.

Krylova EM. 2001. Septibranchiate molluscs of the family Poromyidae (Bivalvia: Poromyoidea) from the tropical western Pacific Ocean. *Mémoires du Muséum National d'Histoire Naturelle, Paris* **185:** 165–200.

Machado FM, Morton B, Passos FD. 2017. Functional morphology of *Cardiomya cleryana* (d'Orbigny, 1842) (Bivalvia: Anomalodesmata: Cuspidariidae) from Brazilian waters: new insights into the lifestyle of carnivorous bivalves. *Journal of the Marine Biological Association of the United Kingdom* **97:** 447–462.

Machado FM, Passos FD. 2015. Spheniopsidae Gardner, 1928 (Bivalvia): conchological characters of two new species from off Brazil, Southwestern Atlantic. *American Malacological Bulletin* **33:** 1–9.

Malkowsky Y, Jochum A. 2014. Three-dimensional reconstructions of pallial eyes in Pectinidae (Mollusca: Bivalvia). *Acta Zoologica* **96:** 167–173.

Mikkelsen PM, Bieler R. 2008. *Seashells of Southern Florida: living marine mollusks of the Florida Keys and adjacent regions: bivalves*. Princeton, NJ: Princeton University Press.

Morton B. 1974. Some aspects of the biology and functional morphology of *Cleidothaerus maorianus* Finlay (Bivalvia: Anomalodesmata: Pandoracea). *Proceedings of the Malacological Society of London* **41:** 201–222.

Morton B. 1981. Prey capture in the carnivorous septibranch *Poromya granulata* (Bivalvia: Anomalodesmata: Poromyacea). *Sarsia* **66:** 241–256.

Morton B. 1982. The functional morphology of *Parilimya fragilis* (Grieg 1920) (Bivalvia: Parilimyidae nov. fam.) with a discussion on the origin and evolution of the carnivorous septibranchs and a reclassification of the Anomalodesmata. *Transactions of the Zoological Society of London* **36:** 153–216.

Morton B. 1984a. Prey capture in *Lyonsiella formosa* (Bivalvia, Anomalodesmata, Verticordiacea). *Pacific Science* **38:** 283–297.

Morton B. 1984b. Adventitious tube construction in *Brechites vaginiferus* (Bivalvia: Anomalodesmata: Clavagellacea) with an investigation of the juvenile of '*Humphreyia strangei*'. *Journal of Zoology, London* **203:** 461–484.

Morton B. 1985. *Adaptive radiation in the Anomalodesmata*. In: Wilbur KM, Trueman ER, Clarke M, eds. *The Mollusca, Vol. 10. Evolution*. New York: Academic Press, 405–459.

Morton B. 1987. Siphon structure and prey capture as a guide to affinities in the abyssal septibranch Anomalodesmata. *Sarsia* **72:** 49–69.

Morton B. 2002. Biology and functional morphology of the watering pot shell *Brechites vaginiferus* (Bivalvia: Anomalodesmata: Clavagelloidea). *Journal of Zoology, London* **257:** 545–562.

Morton B. 2010. Form and functional morphology of *Raetellops pulchella* (Bivalvia: Mactridae): an example of convergent evolution with the Anomalodesmata. *Invertebrate Biology* **129:** 241–251.

Morton B, Machado FM, Passos FD. 2016a. The smallest carnivorous bivalve? Biology, morphology and behaviour of *Grippina coronata* (Anomalodesmata: Cuspidarioidea: Spheniopsidae) preying on epipsammic microcrustaceans in the southwestern Atlantic off Brazil. *Journal of Molluscan Studies* **82:** 244–258.

Morton BS, Prezant RS, Wilson B. 1998. *Class Bivalvia*. In: Beesley PL, Ross GJB, Wells A, eds. *Mollusca: The southern synthesis. Fauna of Australia,* **Vol. 5**. Melbourne: CSIRO Publishing, 195–234.

Morton B, Machado FM, Passos FD. 2016b. The organs of prey capture and digestion in the miniature predatory bivalve *Spheniopsis brasiliensis* (Anomalodesmata: Cuspidarioidea: Spheniopsidae) expose a novel life-history trait. *Journal of Natural History* **50:** 1725–1748.

Morse MP, Zardus JD. 1997. Bivalvia. In: Harrison FW, Kohn AJ, eds. *Microscopic anatomy of invertebrates. Vol. 6A, Mollusca II*. New York: Wiley–Liss, 7–118.

Narchi W. 1968. The functional morphology of *Lyonsia californica* Conrad, 1837. *Veliger* **10:** 305–313.

Palmer BA, Taylor GJ, Brumfeld V, Gur D, Shemesh M, Elad N, Osherov A, Oron D, Weiner S, Addadi L. 2017. The image-forming mirror in the eye of the scallop. *Science* **358:** 1172–1175.

Parapar J, Candás M, Cunha-Veira X, Moreira J. 2017. Exploring annelid anatomy using micro-computed tomography: a taxonomic approach. *Zoologischer Anzeiger* **270:** 19–42.

Pelseneer P. 1911. *Les Lamellibranches de l'expédition du Siboga: partie anatomique. Siboga-Expeditie: uitkomsten op zoölogisch, botanisch, oceanographisch en geologisch gebied verzameld in Nederlandsch Oost-Indië 1899–1900 aan boord H.M. Siboga onder commando van Luitenant ter Zee 1e kl. G.F. Tydeman, 53a*. Leiden: Boekhandel en drukkerij, 1–125.

Predouzo L, García-Álvarez Ó, Urgorri V, Pérez-Señarís M. 2017. New data and 3D reconstructions of four species of Pruvotinidae (Mollusca: Solenogastres) from the NW Iberian Peninsula. *Marine Biodiversity.* doi: 10.1007//s12526-017-0793-1.

Purchon RD. 1956. The stomach in the Protobranchia and Septibranchia (Lamellibranchia). *Proceedings of the Zoological Society of London* **127:** 511–525.

Purchon RD. 1959. Phylogenetic classification of the Lamellibranchia, with special reference to the Protobranchia. *Proceedings of the Malacological Society* **33:** 224–230.

Purchon RD. 1960. Phylogeny in the Lamellibranchia. In: Purchon RD, ed. *Proceedings of the centenary and bicentenary congress of Biology, Singapore, Dec. 1958*. Singapore: University of Malaya Press, 69–82.

Purchon RD. 1963. Phylogenetic classification of the Bivalvia, with special reference to the Septibranchia. *Proceedings of the Malacological Society* **35:** 71–80.

Purchon RD. 1987. The stomach in the Bivalvia. *Philosophical Transactions of the Royal Society of London, Series B: Biological Sciences* **316:** 183–276.

Purchon RD. 1990. Stomach structure, classification and evolution of the Bivalvia. In: Morton B, eds. *The Bivalvia – proceedings of a memorial symposium in honour of Sir Charles Maurice Yonge, 1986*. Hong Kong: Hong Kong University Press, 73–95.

Simone RL, Cunha MC. 2008. Revision of the genus *Spinosipella* (Bivalvia: Verticordiidae), with a description of two new species from Brazil. *The Nautillus* **122:** 57–78.

Stasek CR. 1963. Synopsis and discussion of the association of ctenidia and labial palps in the bivalved Mollusca. *Veliger* **6:** 91–97.

Tëmkin I, Strong EE. 2013. New insights on stomach anatomy of carnivorous bivalves. *Journal of Molluscan Studies* **79:** 332–339.

Tessler M, Barrio A, Borda E, Rood-Goldman R, Hill M, Siddall ME. 2016. Description of a soft-bodied invertebrate with microcomputed tomography and revision of the genus *Chtonobdella* (Hirudinea: Haemadipsidae). *Zoologica Scripta* **45:** 552–565.

Thiele J. 1912. Die antarktischen Schnecken und Muscheln. Deutsche Südpolar-Expedition 1901–1903. *Wissenschaftliche Ergebnisse. 13, Zoologie* **5:** 185–285, pls. 18.

Yonge CM. 1928. Structure and function of the organs of feeding and digestion in the septibranchs, *Cuspidaria* and *Poromya*. *Philosophical Transactions of the Royal Society of London, Series B* **216:** 221–263.

Yonge CM. 1952. Structure and adaptation in *Entodesma saxicola* (Baird) and *Mytilimeria nuttallii* Conrad. *University of California Publications in Zoology* **55:** 439–450.

Yonge CM. 1982. Mantle margins with a revision of siphonal types in the Bivalvia. *Journal of Molluscan Studies* **48:** 102–103.

Ziegler A, Menze BH. 2013. Accelerated acquisition, visualization, and analysis of zoo-anatomical data. In: Zander J, Mosterman PJ, eds. *Computation for humanity. information technology to advance society*. Boca Raton: CRC Press, 233–260.